



저작자표시-비영리-변경금지 2.0 대한민국

이용자는 아래의 조건을 따르는 경우에 한하여 자유롭게

- 이 저작물을 복제, 배포, 전송, 전시, 공연 및 방송할 수 있습니다.

다음과 같은 조건을 따라야 합니다:



저작자표시. 귀하는 원저작자를 표시하여야 합니다.



비영리. 귀하는 이 저작물을 영리 목적으로 이용할 수 없습니다.



변경금지. 귀하는 이 저작물을 개작, 변형 또는 가공할 수 없습니다.

- 귀하는, 이 저작물의 재이용이나 배포의 경우, 이 저작물에 적용된 이용허락조건을 명확하게 나타내어야 합니다.
- 저작권자로부터 별도의 허가를 받으면 이러한 조건들은 적용되지 않습니다.

저작권법에 따른 이용자의 권리는 위의 내용에 의하여 영향을 받지 않습니다.

이것은 [이용허락규약\(Legal Code\)](#)을 이해하기 쉽게 요약한 것입니다.

[Disclaimer](#)

의학박사 학위논문

**Role of tumor immune
microenvironment in progression of
ductal carcinoma in situ of the breast**

유방 관상피내암종의 진행에 관련된
종양 면역미세환경의 역할

2021년 2월

서울대학교 대학원
의학과 병리학 전공
김 미 립


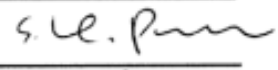

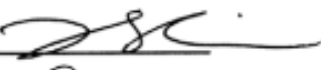
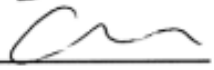
Role of tumor immune microenvironment in progression of ductal carcinoma in situ of the breast

October 2020

**Graduate School of Medicine
Seoul National University**

Milim Kim

**Confirming the Ph.D. Dissertation written by
Milim Kim
January 2012**

Chair	<u>GHEEYOUNG CHOE </u>
Vice Chair	<u>So Yeon Park </u>
Examiner	<u>Hye Seung Lee </u>
Examiner	<u>Jee Hyun Kim </u>
Examiner	<u>Eun Yoon Cho </u>


유방 관상피내암종의 진행에 관련된 종양 면역미세환경의 역할

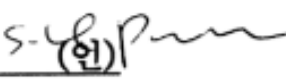
지도교수 박 소 연


이 논문을 의학박사 학위논문으로 제출함
2020년 10월


서울대학교 대학원
의학과 병리학전공
김 미 립

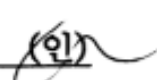
김미립의 의학박사 학위논문을 인준함
2021년 1월

위원장 최 기 영  (인)

부위원장 박 소 연  (인)

위원 이 혜 승  (인)

위원 김 지 현  (인)

위원 조 은  (인)

Abstract

Milim Kim

Department of Medicine, Pathology Major

Graduate School of Medicine

Seoul National University

Background: The immune microenvironment of ductal carcinoma in situ (DCIS) and its significance are not well established. This study was conducted to evaluate the role of immune microenvironment during progression of DCIS by examining composition of tumor infiltrating lymphocyte (TIL) subsets, PD-L1+ immune cells infiltration and immune-related gene expression in DCIS, compared to those of invasive carcinoma of the breast.

Materials and Methods: Three different groups of breast cancer samples including pure DCIS, DCIS with microinvasion (DCIS-M), and invasive carcinoma were used in this study. CD4+, CD8+, and FOXP3+ TIL subsets and PD-L1+ immune cells were detected with immunohistochemistry using tissue microarrays. By immune profiling using Nanostring nCounter platform, CXCL10 was detected as the most differentially expressed gene, and its expression was validated in DCIS and invasive carcinoma using real-time polymerase chain reaction and immunohistochemistry. CXCL10 expression and its relation with clinicopathologic characteristics of tumors and infiltration of immune cell subset infiltration were also analyzed.

Results: All immune cell infiltrations were higher in invasive carcinoma than in pure DCIS regardless of hormone receptor (HR) status. Within individual cases of invasive carcinoma with DCIS component, all immune cell subset infiltration was higher in the invasive component than in DCIS component; however, CD4+ TIL

infiltration did not differ between the two components in HR-negative tumors. Comparing pure DCIS, DCIS-M, and DCIS associated with invasive carcinoma (DCIS-INV), CD4⁺ TIL infiltration revealed a gradual increase from pure DCIS to DCIS-M and DCIS-INV in HR-negative group, whereas FOXP3⁺ TIL infiltration was significantly increased in DCIS-INV than pure DCIS in HR-positive group. High infiltration of FOXP3⁺ TIL and the presence of PD-L1⁺ immune cells were associated with tumor recurrence in patients with pure DCIS. CXCL10 mRNA expression was significantly higher in invasive carcinoma than in DCIS, in the whole groups and in the HR-negative subgroup. Its expression was also significantly higher in DCIS-INV than in DCIS, especially in HR-negative tumors. Moreover, CXCL10 mRNA expression showed positive correlation with TIL density in both DCIS and invasive carcinoma, and CXCL10-positive tumors generally showed higher infiltration of CD8⁺ and FOXP3⁺ TILs, and PD-L1⁺ immune cells compared to CXCL10-negative tumors, albeit with different patterns according to HR status.

Conclusions: This study showed that immune microenvironment differs significantly between pure DCIS, DCIS-INV and invasive carcinoma in terms of immune cell subset infiltration depending on HR status, and CXCL10 expression is associated with difference in immune cell infiltration between DCIS and invasive carcinoma, implying their roles in the progression of DCIS to invasive carcinoma.

Keyword: ductal carcinoma in situ; invasive breast cancer; tumor immune microenvironment; tumor infiltrating lymphocyte; CXCL10

Student Number: 2016-27715

Table of Contents

Abstract	i
Table of Contents	iii
List of Tables	iv
List of Figures.....	vi
List of Supplementary Tables	vii
List of Abbreviations.....	ix
Introduction	1
Materials and Methods.....	4
Results	16
Discussion	43
Conclusion.....	52
Bibliography	66
Abstract in Korean	70

List of Tables

Table 1. Clinicopathologic characteristics of pure DCIS and DCIS with microinvasion (set 1).....	7
Table 2. Relationship between immune cell subset infiltration and clinicopathologic features of pure DCIS.....	18
Table 3. Comparison of immune cell subset infiltration in pure DCIS and invasive carcinoma.....	20
Table 4. Comparison of CD4+ and CD8+ tumor infiltrating lymphocyte infiltration in individual tumors.....	21
Table 5. Comparison of immune cell infiltration in the DCIS and invasive components of individual tumors	24
Table 6. Comparison of infiltration of immune cell subsets in pure DCIS, DCIS with microinvasion, and DCIS associated with invasive carcinoma	26
Table 7. List of top 20 genes with significant fold change between DCIS and invasive carcinoma.....	31
Table 8. Comparison of CXCL10 mRNA expression between DCIS and invasive carcinoma.....	33
Table 9. Comparison of CXCL10 mRNA expression between DCIS and DCIS associated with invasive carcinoma	34
Table 10. Comparison of CXCL10 mRNA expression in DCIS and invasive components of individual tumors	36

Table 11. Comparison of immune cell subset infiltration in relation to CXCL10 expression in DCIS and invasive carcinoma.....	42
--	----

List of Figures

Figure 1. Representative example of CD4+, CD8+ and FOXP3+ tumor-infiltrating lymphocytes and PD-L1+ immune cell infiltration in pure DCIS	17
Figure 2. Representative example of CD4+, CD8+ and FOXP3+ tumor-infiltrating lymphocytes and PD-L1+ immune cell infiltration in in situ and invasive component	22
Figure 3. Kaplan-Meier survival curve stratified by immune cell subset infiltration and their ratio in pure DCIS	28
Figure 4. Volcano plot showing difference of CXCL10 expression between DCIS and invasive carcinoma	30
Figure 5. Correlation between tumor infiltrating lymphocytes and CXCL10 mRNA fold change ($2^{-\Delta\Delta C_t}$) in DCIS and invasive carcinoma	37
Figure 6. Representative example of CXCL10 expression in DCIS and invasive carcinoma.....	39
Figure 7. Comparison of CXCL10 expression between DCIS and invasive carcinoma	40

List of Supplementary Tables

Supplementary Table S1. Correlations in infiltration of CD4+, CD8+, and FOXP3+ tumor infiltrating lymphocytes and PD-L1+ immune cells (ICs) in pure DCIS.....	54
Supplementary Table S2. Summary of 6 cases with ipsilateral breast recurrence	55
Supplementary Table S3. Clinicopathologic characteristics of DCIS (set 2)	56
Supplementary Table S4. Clinicopathologic characteristics of Invasive Carcinoma (set 2).....	57
Supplementary Table S5. List of top 20 genes with significant fold change between DCIS and invasive carcinoma in ER-positive tumors.....	58
Supplementary Table S6. List of top 20 genes with significant fold change between DCIS and invasive carcinoma in ER-negative tumors.....	59
Supplementary Table S7. Clinicopathologic characteristics of DCIS (set 3)	60
Supplementary Table S8. Clinicopathologic characteristics of invasive carcinoma (set 3).....	61
Supplementary Table S9. Clinicopathologic characteristics of DCIS (set 4)	62
Supplementary Table S10. Clinicopathologic characteristics of invasive carcinoma (set 4).....	63

Supplementary Table S11. Relationship between CXCL10 expression and clinicopathologic features of DCIS.....	64
---	----

Supplementary Table S12. Relationship between CXCL10 expression and clinicopathologic features of invasive carcinoma.....	65
---	----

List of Abbreviations

CTL	cytotoxic T lymphocyte
DCIS	ductal carcinoma in situ
DCIS-M	DCIS with microinvasion
DCIS-INV	DCIS associated with invasive carcinoma
ER	estrogen receptor
HER2	human epidermal growth factor receptor 2
HR	hormone receptor
IC	immune cell
PCR	polymerase chain reaction
PD-L1	programmed death-ligand 1
PR	progesterone receptor
TIL	tumor infiltrating lymphocyte

1. Introduction

Ductal carcinoma in situ (DCIS) is an early pathologic stage of breast cancer characterized by proliferation of tumor cells within the ductal-lobular unit. Introduction of screening mammography has resulted in increased detection of DCIS which currently accounts for 20~25% of newly diagnosed breast cancers in USA [1]. DCIS is a non-obligatory precursor of invasive breast cancer that progresses to invasive cancer over 10-15 years in 14-53% [2]. The mechanism by which DCIS progresses to invasive carcinoma is not well understood, but it is thought to be a complex process driven by tumor cells (through genetic aberrations or altered expression of genes critical for invasion) and tumor microenvironment including myoepithelial cells, stromal fibroblasts, and immune infiltrates [3].

The immune system can eliminate tumor cells or control tumor growth by immune surveillance, but interaction between tumor cells and the immune system is known to play a crucial role in tumor progression [4]. Key players of the immune system include myeloid cells, lymphocytes, cytokines, and chemokines of which tumor infiltrating lymphocytes (TILs) are thought to represent tumor immunogenicity, and their composition is associated with the direction of an immune response [5, 6].

Studies to date generally agree that CD8⁺ cytotoxic T lymphocytes (CTLs) and CD4⁺ Th1 cells are involved in effective anti-tumor immunity while FOXP3⁺ regulatory T cells are associated with suppression of anti-tumor immunity [7]. Besides TILs, immune checkpoint molecules are also involved in regulation of anti-tumor responses. Especially, programmed death-ligand 1 (PD-L1), also known as B7-H1 or CD274, is expressed on tumor cells and immune cells; it suppresses T-

cell migration, proliferation, and secretion of cytotoxic mediators, and it also restricts tumor cell killing through binding to programmed death-1 (PD-1) and B7.1 (CD80) [8].

Most of the previous studies on TILs and their composition in breast cancer have focused on their predictive and prognostic significance in invasive breast cancer [9-14]; their presence and significance in DCIS remain elusive. A few studies have reported that dense TILs in DCIS were associated with more aggressive clinical features and an increased risk to progression [15, 16], and specific TIL subsets in DCIS have been linked to tumor recurrence [17-19]. However, there is a lack of studies on TIL subset infiltration in DCIS and its comparison with that of invasive breast cancer. Moreover, only a few studies have evaluated PD-L1+ immune cells in DCIS with a limited number of cases [16, 20-22].

Chemokines are small proteins, usually between 8 to 10 kDa, known to provide directional cues for leukocytes in development, homeostasis and inflammation through interaction with a subset of seven-transmembrane G protein-coupled receptors (GPCRs) [23]. Their role as a pro-inflammatory mediator that attracts leukocyte at the site of inflammation is well elucidated and chemokines have been considered a potential target for inflammatory diseases and autoimmune diseases [24, 25]. Aside from its role in inflammation, chemokines are also involved in tumor progression and metastasis through different mechanisms; cancer cell attraction to site of metastasis, mobilization of bone marrow-derived leukocytes, including regulatory T cells, myeloid derived suppressor cells and tumor associated macrophages, and autocrine signaling for tumor growth [25]. However, in breast cancer, understanding of the role of chemokine in tumorigenesis

and tumor progression is limited.

Since the interaction between tumor cells and the immune microenvironment plays an essential role in tumor progression, elucidating the difference in the immune microenvironment between DCIS and invasive carcinoma may help to understand the mechanisms underlying progression of DCIS. In this study, the infiltrations of CD4+, CD8+, and FOXP3+ TILs, and PD-L1+ immune cells were examined in DCIS in relation to clinicopathologic features, and they were compared with those of invasive breast cancer to evaluate their changes during progression of DCIS. Moreover, immune-related genes including chemokines that were differentially expressed between DCIS and invasive carcinoma were identified to further characterize what causes differences in tumor microenvironment. In addition, real time polymerase chain reaction and immunohistochemistry was performed to validate the difference of the selected immune-related genes between DCIS and invasive carcinoma.

2. Materials and Methods

2.1. Comparison of immune cell subset infiltration between DCIS and invasive carcinoma

2.1.1. Study population

A total of 671 cases (set 1), comprising 231 cases of pure DCIS, 81 cases of DCIS with microinvasion (DCIS-M), and 359 cases of invasive breast carcinoma that have been diagnosed between 2003 and 2011 at Seoul National University Bundang Hospital were used. In a previous study, 377 cases of invasive breast carcinoma had been used for evaluation of TIL subsets infiltration except for PD-L1 [14]. After excluding 18 cases of invasive lobular carcinoma, the data of the remaining 359 invasive carcinomas was used for this study. Of the 259 invasive carcinoma cases, ninety cases which had a sufficient amount of DCIS component associated with invasive carcinoma were selected for comparative analysis of the invasive and DCIS components within the same tumor.

2.1.2. Tissue microarrays (TMAs)

H&E-stained slides from formalin-fixed, paraffin-embedded tissue blocks were reviewed, and representative sections were selected in each case for construction of tissue microarrays (TMAs). For ductal carcinoma in situ and microinvasive carcinomas, one to three tissue columns of 4 mm-diameter circles (depending on the extent of the tumor) were arranged in TMA using a trephine apparatus (Superbiochips Laboratories, Seoul, Korea). For invasive carcinoma, three sets of TMAs (2 mm in diameter) that had been constructed for the previous study [14] were used. For comparative analysis between invasive and DCIS components of

the same tumor, one tissue column of DCIS associated with invasive carcinoma (DCIS-INV) (4 mm in diameter) was selected and was made into TMAs.

2.1.3. Clinicopathologic information

Clinicopathologic information was obtained by reviewing medical records and hematoxylin and eosin (H&E)-stained sections. For pure DCIS and DCIS-M, clinicopathologic data including patient age, tumor extent, nuclear grade, presence of comedo-type necrosis, architectural pattern, presence of microinvasive foci, estrogen receptor (ER), progesterone receptor (PR), human epidermal growth factor receptor 2 (HER2) status, Ki-67 proliferation index, and p53 overexpression were recorded. Baseline characteristics of pure DCIS and DCIS-M are summarized in **Table 1**. These two groups were significantly different in various clinicopathologic characteristics including DCIS extent, nuclear grade, ER, PR and HER2 status.

2.1.4. Immunohistochemistry for immune cells and counting

Immunohistochemical staining was performed with a BenchMark XT autostainer (Ventana Medical Systems) using an UltraView detection kit (Ventana Medical Systems) for CD4, CD8, FOXP3, and PD-L1. The following antibodies were used: CD4 (Clone SP35; ready to use; Dako), CD8 (Clone C8/144B; ready to use; Dako), FOXP3 (Clone 236A/E7; 1:100 dilution; Abcam, Cambridge, United Kingdom), and PD-L1 (clone E1L3N; 1:100 dilution; Cell Signaling, Danvers, MA).

For evaluation of CD4+, CD8+, and FOXP3+ T cell infiltration, the number of each TIL subset was counted by two pathologists who were blinded to the clinicopathologic features of the tumors. From the TMA cores, three areas with the

highest infiltration were chosen under the high-power field (400X), and the number of TIL subset was counted in both intra-tumoral and stromal compartments either manually or using a digital image analyzer, ScanScope CS system (Aperio, Vista, CA). Then, the average number of CD4+, CD8+, and FOXP3+ T cells from the selected areas were calculated. In cases of DCIS, stromal compartment was defined as the area of the specialized stroma surrounding the involved ducts, or when it is not clear, as an area surrounding ducts within 2 high-power fields according to a proposal from the International Immuno-Oncology Biomarker Working Group [26, 27]. As for PD-L1, PD-L1+ immune cells were considered to be present when at least 1% of the tumor stromal area was occupied by PD-L1+ immune cells, as previously described [16].

Table 1. Clinicopathologic characteristics of pure DCIS and DCIS with microinvasion (set 1)

Clinicopathologic characteristics		Pure DCIS (<i>n</i> =231)	DCIS with microinvasion (<i>n</i> =81)	<i>p</i> -value
Age (years)	Median (range)	47 (25-88)	48 (26-76)	0.556
Extent of DCIS (cm)	Median (range)	2.5 (0.4-12.2)	4.2 (0.9-14.5)	<0.001
Nuclear grade	Low	16 (6.9)	2 (2.5)	<0.001
	Intermediate	129 (55.8)	20 (24.7)	
	High	86 (37.2)	59 (72.8)	
Comedo-type necrosis	Absent	181 (78.4)	30 (37.0)	<0.001
	Present	50 (21.6)	51 (63.0)	
ER	Negative	30 (13.0)	42 (51.9)	<0.001
	Positive	201 (87.0)	39 (48.1)	
PR	Negative	44 (19.0)	47 (58.0)	<0.001
	Positive	187 (81.0)	34 (42.0)	
HER2	Negative	196 (84.8)	43 (53.1)	<0.001
	Positive	35 (15.2)	38 (46.9)	
Ki-67 index	<10%	171 (74.0)	30 (37.0)	<0.001
	≥10%	60 (26.0)	51 (63.0)	
P53	Negative	201 (87.0)	51 (63.0)	<0.001
	Positive	30 (13.0)	30 (37.0)	

p-values were calculated by Mann-Whitney U test and chi-square or Fisher's exact test.

Numbers in parentheses indicate column percentage.

2.2. Immune profiling using Nanostring nCounter assay

2.2.1. Study population and RNA extraction

Breast cancers that have been resected between 2009 and 2012 at Seoul National University Bundang Hospital were selected for Nanostring nCounter assay. A total of 48 cases of tissue specimens (16 cases of DCIS and 32 cases of invasive carcinoma; set 2) with sufficient amount of tumor that were well fixed were chosen for analysis. Clinicopathologic data of these samples are summarized in **Supplementary Table S3 and S4**. Using 10µm thick sections of FFPE tissue, RNA was extracted using RecoverAll™ Total Nucleic Acid Isolation Kit (Ambion, Grand Island, NY). Concentration of extracted RNA were determined using DS-11 Spectrophotometer (Denovix INC, Wilmington, DE) and RNA quality check was done using Fragment Analyzer (Advanced Analytical Technologies, Ankeny, IA). Of 48 cases, one case with low RNA concentration was excluded for final analysis.

2.2.2. mRNA expression and nCounter data analysis

For the analysis of mRNA expression using the above sample, a digital multiplexed nanoString nCounter human mRNA expression assay (NanoString Technologies, Seattle, WA) was performed with human Immune Profile Panel Kit, which includes 770 immune-related gene and control genes, according to the manufacturer's protocol. Target molecules were quantified by the nCounter Digital Analyzer by counting the individual fluorescent barcodes. For each assay, a high-density scan encompassing 280 fields of view was performed. The Data was collected using the nCounter Digital Analyzer after taking images of the immobilized fluorescent reporters in the sample cartilage with CCD camera.

2.3. Validation of a differentially expressed immune-related gene, CXCL10 in DCIS and invasive carcinoma

2.3.1. Study population and evaluation of TILs

A total of 120 cases (set 3) that were diagnosed and operated between 2009 and 2012 at Seoul National University Bundang Hospital were used. Of 120 cases, 60 cases were invasive carcinoma, and 60 cases were DCIS (39 cases, pure DCIS; 21 cases, DCIS-M). Clinicopathologic characteristics are summarized in **Supplementary Table S7 and S8**. Of the 60 invasive carcinoma cases, 24 cases which had a sufficient amount of DCIS component were selected for comparative analysis of the invasive component and DCIS components within the same tumor.

On H&E-stained sections, the average percentage of TILs in stromal component were evaluated using 10% increment. Areas with TILs less than 10% were assessed as either 1% or 5%. In DCIS, stromal compartment was defined according to a proposal from Immuno-Oncology Biomarker Working Group [26, 27]

2.3.2. RNA isolation, mRNA reverse transcription and real-time quantitative PCR

Representative paraffin blocks from each cases were selected, two to three serial sections (10 μ m thick) were cut, and tumor areas comprised with more than 70% of tumor cells were marked and manually dissected. Total RNA was extracted using RNeasy FFPE Kit (Qiagen, Hilden, Germany) according to manufacturer's instructions. High capacity RNA-to-cDNA kit (Applied Biosystems, Foster City, CA) protocol was used to transcribe total RNA into single-stranded cDNA. For

real-time polymerase chain reaction (PCR), we used TaqMan Gene Expression Assay for both CXCL10 and the human glyceraldehyde-3-phosphate dehydrogenase (GAPDH), as well as TaqMan Universal PCR Mastermix (Applied Biosystems). Real-time PCR was performed using a StepOne Real-Time PCR systems (Applied Biosystems). The reaction incubated at 95°C for 10 minutes, followed by 50 cycles at 95°C for 15 seconds, 60°C for 1 minute. The human glyceraldehyde-3-phosphate dehydrogenase (GAPDH) was used in each plate as control.

CXCL10 mRNA expression was calculated using comparative Ct method (Δ Ct). The threshold cycle (Ct) of CXCL10 was measured and the data were normalized by subtracting the Ct value of an endogenous reference, GAPDH. For comparison of Δ Ct value of mRNA of breast cancer with that of normal breast tissue, normalized Δ Ct values were measured from 15 normal breast tissue samples excised for reduction mammoplasty. The average Δ Ct value of benign breast tissue was used to calculate normal Δ Ct value, and the average of this value was subtracted from Δ Ct of CXCL10 treated samples to determine differences ($\Delta\Delta$ Ct) and fold change ($2^{-\Delta\Delta\text{Ct}}$). For data that are proven to have sufficient amount of RNA and Ct value for housekeeping gene but had non-detectable Ct value for CXCL10, after repeated non-detection of samples, the maximum number of PCR cycle, 50, was used as Ct value of each sample according to Applied Biosystem DataAssist v.3.0 software.

2.4. Evaluation of CXCL10 expression and its association with immune cell subset infiltration in breast cancer

2.4.1. Study population

A total of 593 cases (set 4) comprised with 223 cases of DCIS including pure DCIS and DCIS-M and 372 cases of invasive carcinoma which were operated at Seoul National University Bundang Hospital from 2003 to 2011 were used in this analysis. Clinicopathologic characteristics of DCIS and invasive carcinoma are presented in **Supplementary Table S9 and S10**. Data of immune cell subset infiltration were from the previous first data set. After excluding missing values, a total of 223 cases of DCIS and 151 cases of invasive carcinoma were used for the comparison of immune cell subset infiltration in relation to CXCL10 expression in tumor area.

2.4.2. Immunohistochemistry and scoring of CXCL10

Representative sections of each case were constructed into tissue microarray as aforementioned. Immunohistochemical staining for CXCL10 was performed on tissue microarrays after staining optimization using positive and negative control (tonsil tissue) and serial dilution. Slides submitted were deparaffinized, and rehydrated in graded ethanol. Antigen retrieval was performed by immersing the slides in citrate buffer (pH 6.0) for 30 minutes in a steamer. Using 3% H₂O₂-methanol solution, endogenous peroxidase activity was blocked and then the slides were incubated in 10% normal goat serum for 30 minutes to prevent non-specific staining. Using anti-IP10 antibody (CXCL10) (polyclonal; 1:500 dilution; Abcam), slides were incubated for 1 hour at room temperature. After, the sections were

incubated with horseradish peroxidase-labeled polymer conjugated with secondary antibodies (DAKO Envision detection kit, Dako) for 30 minutes. Diaminobenzidine was used as a chromogen, and sections were counterstained with Mayer's hematoxylin.

Expression of CXCL10 in tumor area, including tumor cells, tumor stromal cells, lymphocytes and macrophages, were evaluated blinded to clinicopathologic information. Positively-stained tumor area with dot-like cytoplasmic or membranous staining pattern were considered positive regardless of staining intensity. CXCL10 was considered to be positive when at least 1% of the tumor area were positively stained.

2.5. Evaluation of basic biomarkers

Expression of the basic biomarkers including ER, PR, HER2, p53, and Ki-67 was evaluated from the surgical specimens at the time of diagnosis. As for those with missing data, immunohistochemical staining on representative tissue sections was carried out using the following antibodies: ER (clone SP1; 1:100 dilution; LabVision, Fremont, CA), PR (clone PgR 636; 1:70 dilution; Dako), HER2 (clone 4B5; ready to use; Ventana Medical Systems, Tuscon, AZ), p53 (clone D07; 1:600 dilution; Dako), and Ki-67 (clone MIB-1; 1:250 dilution; Dako).

ER and PR were regarded as positive if at least 1% of the tumor cells were stained. HER2 positivity was defined as an immunohistochemical score of 3+ or the presence of gene amplification on fluorescence/silver in situ hybridization. For p53, staining in 10% or more of the tumor cells was considered positive. High Ki-67 proliferation index was defined as staining in 10% or more of the tumor cells in

DCIS and DCIS-M and a cut off value of 10% or 20% were used for invasive carcinomas.

2.6. Statistical analysis

2.6.1. Immune cell subsets

Statistical analysis was performed using Statistical package, SPSS version 25.0 for Windows (IBM Corp., Armonk, NY). CD4+, CD8+, and FOXP3+ TIL counts did not show normal distributions and thus, non-parametric tests were used for statistical analyses. Spearman's rank correlation tests were used to assess the associations among infiltrations of CD4+, CD8+, and FOXP3+ TILs and PD-L1+ immune cells. The difference in infiltration of CD4+, CD8+, and FOXP3+ TILs was analyzed by Mann-Whitney U test between two groups, and by Kruskal-Wallis test among three groups. For detection of the predominant TIL subset in the same disease group or for comparison of TIL subset infiltration between invasive and in situ components in the same tumor, Wilcoxon signed rank test was used. Presence or absence of PD-L1+ immune cells were analyzed by chi-square test between groups, and its comparison between invasive and in situ components in the same tumor was performed using McNemar test. In pure DCIS, a receiver operating characteristic (ROC) curve analysis was performed to identify the cut-off values for CD4+, CD8+, and FOXP3+ TILs and ratios of TIL subsets (FOXP3+/CD8+ TIL, FOXP3+/CD4+ TIL and CD4+/CD8+ TIL) that maximized the sum of sensitivity and specificity in predicting ipsilateral breast cancer recurrence using recurrence as a dichotomous outcome. Recurrence-free survivals were analyzed by drawing Kaplan-Meier curves, and differences were determined with the log-rank test.

When comparing immune cell subset infiltration among pure DCIS, DCIS-M, and DCIS-INV, corrections for multiple testing were made by Bonferroni method, and adjusted (adj.) *p*-values were calculated. *P*-values less than 0.05 were considered significant with all reported *p*-values being two-sided.

2.6.2. nCounter data analysis

Analysis of raw mRNA data was performed using NanoString technologies nSolver analysis software version 4.0. The mRNA expression data was normalized using housekeeping genes. R software was used for comparison of mRNA expression between two groups. Difference in gene expression between DCIS and invasive carcinoma were presented as Log2 fold change, and *p*-value was adjusted by Benjamini-Yekutieli procedure

2.6.3. Real-time PCR of CXCL10

Fold change ($2^{-\Delta\Delta Ct}$) of all groups, including DCIS, invasive carcinoma, and DCIS-INV, did not show normal distribution and thus non-parametric tests were used for analysis. For comparison of CXCL10 fold change between DCIS and invasive carcinoma as well as DCIS and DCIS-INV, Mann-Whitney U test was used. For the comparison of CXCL10 expression between invasive component and in situ components in the same tumor, Wilcoxon signed rank test was used. In order to evaluate correlation between CXCL10 mRNA expression and TILs in both DCIS and invasive carcinoma, spearman's rank correlation test was used. *P*-values less than 0.05 were considered significant for all cases.

2.6.4. Expression of CXCL10 and its association with immune cell subset infiltration

Chi-square and Fisher's exact tests were used to evaluate CXCL10 expression in relation to clinicopathologic features of DCIS and invasive carcinoma. Mann-Whitney U test were used to analyze CD4+, CD8+, and FOXP3+ TILs and PD-L1+ immune cell infiltration in relation to CXCL10 expression. *P*-values less than 0.05 were considered significant.

3. Results

3.1 Immune cell subset infiltration in DCIS, DCIS-M and IC

3.1.1 Infiltration of immune cell subsets and their relationship with clinicopathologic features of pure DCIS

In pure DCIS, immune cell infiltration was usually observed in the peri-tumoral specialized stroma surrounding the involved ducts (**Figure 1**). CD4+, CD8+, FOXP3+ TILs, and PD-L1+ immune cells were found within tumors in rare numbers. Infiltration of CD4+, CD8+, and FOXP3+ TILs was quite variable, and they were present in 90.2%, 99.1%, and 30.9% of total cases, respectively. The median numbers of CD4+ and CD8+ TILs were 17.8 (range, 0-279) and 12.5 (range, 0-171) per high-power field. The number of tumor infiltrating FOXP3+ T cells ranged from 0 to 30 under the high-power field. PD-L1 expression in tumor cells was rarely observed with focal positivity in three cases of high-grade DCIS. PD-L1+ immune cells were observed in 15.4% of total cases. Infiltrations of CD4+, CD8+, and FOXP3+ TILs and PD-L1+ immune cells moderately correlated with one another ($\rho=0.310\sim0.566$; $p<0.001$; **Supplementary Table S1**)

First, the relationship between immune cell subset infiltration and clinicopathologic features of pure DCIS was analyzed (**Table 2**). High infiltration of CD4+, CD8+, FOXP3+ TILs, and the presence of PD-L1+ immune cells were commonly associated with high nuclear grade, comedo-type necrosis, ER negativity, PR negativity, and high Ki-67 index (all $p<0.05$). In addition, high infiltration of CD8+ and FOXP3+ TIL was associated with HER2 positivity ($p=0.010$, $p=0.004$, respectively), and infiltration of CD4+, CD8+, and FOXP3+

TILs was higher in tumors with p53 overexpression ($p=0.001$, $p=0.041$, $p=0.016$, respectively).

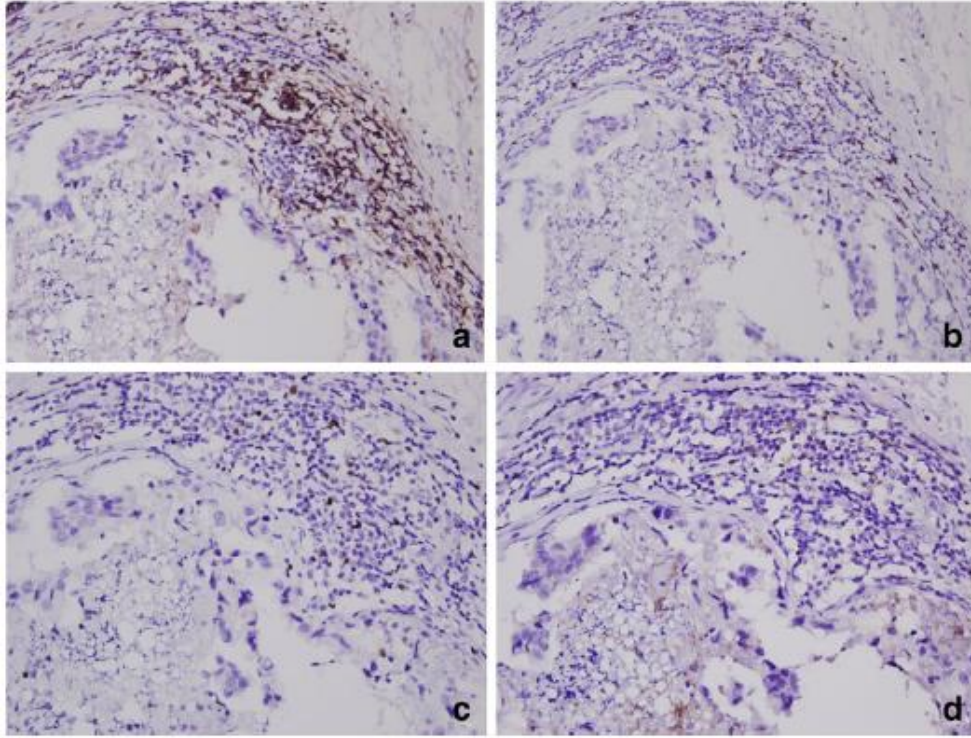


Figure 1. Representative example of CD4+, CD8+, and FOXP3+ tumor-infiltrating lymphocytes and PD-L1+ immune cell infiltration in pure ductal carcinoma in situ. CD4+ (a), CD8+ (b), and FOXP3+ tumor-infiltrating lymphocytes (c) and PD-L1+ immune cells (d) are predominantly found in the peri-tumoral specialized stroma around the involved ducts and are detected in rare numbers within tumor nests.

Table 2. Relationship between immune cell subset infiltration and clinicopathologic features of pure DCIS

Clinicopathologic characteristics	CD4+ TIL		CD8+ TIL		FOXP3+ TIL		PD-L1+ IC	
	No. of TILs	<i>p-value</i>	No. of TILs	<i>p-value</i>	No. of TILs	<i>p-value</i>	Frequency (%)	<i>p-value</i>
Age (year)		0.577		0.218		0.815		0.792
<50	19.7 (4.2-50.7)		12.7 (6.2-26.7)		0.0 (0.0-1.0)		21/132 (15.9)	
≥50	19.0 (3.8-44.5)		12.0 (4.2-22.2)		0.0 (0.0-1.0)		13/89 (14.6)	
DCIS extent (cm)		0.950		0.799		0.811		0.929
<2.5	19.7 (5.0-47.5)		12.7 (5.3-24.2)		0.0 (0.0-1.0)		21/138 (15.2)	
≥2.5	17.3 (3.7-49.7)		11.3 (5.0-26.2)		0.0 (0.0-1.0)		13/83 (15.7)	
Nuclear grade		<0.001		0.001		<0.001		<0.001
Low to intermediate	12.7 (2.0-37.5)		10.0 (4.7-18.2)		0.0 (0.0-0.0)		11/142 (7.7)	
High	25.3 (11.5-77.8)		15.7 (8.0-35.8)		0.0 (0.0-3.0)		23/79 (29.1)	
Comedo-type necrosis		0.004		0.002		0.008		<0.001
Absent	16.0 (3.4-42.0)		10.7 (5.3-20.1)		0.0 (0.0-0.0)		17/174 (9.8)	
Present	31.5 (13.6-86.1)		22.5 (8.5-41.5)		0.0 (0.0-5.0)		17/47 (36.2)	
ER		0.026		0.025		0.004		0.043
Negative	34.0 (13.6-82.4)		22.5 (7.6-48.8)		0.5 (0.0-5.0)		8/27 (29.6)	
Positive	17.0 (3.7-43.5)		11.8 (5.3-22.0)		0.0 (0.0-0.0)		26 /194 (13.4)	
PR		0.027		<0.001		0.002		0.019
Negative	34.0 (12.1-76.3)		24.2 (10.2-48.9)		0.0 (0.0-4.9)		11/40 (27.5)	
Positive	16.0 (3.7-42.0)		10.7 (4.7-19.5)		0.0 (0.0-0.0)		23/181 (12.7)	
HER2		0.354		0.010		0.004		0.059
Negative	17.3 (3.8-44.5)		12.0 (5.2-22.0)		0.0 (0.0-0.0)		25/189 (13.2)	
Positive	28.7 (6.8-73.2)		22.0 (7.3-48.5)		0.0 (0.0-5.2)		9/32 (28.1)	
Ki-67 index		0.001		0.009		<0.001		<0.001
<10%	15.8 (3.4-40.1)		11.0 (4.9-20.2)		0.0 (0.0-0.0)		17/164 (10.4)	
≥10%	34.8 (9.3-96.2)		16.2 (8.3-36.3)		0.0 (0.0-5.0)		17/57 (29.8)	
P53		0.001		0.041		0.016		0.092
Negative	16.3 (3.7-40.4)		11.5 (4.9-22.4)		0.0 (0.0-0.1)		26/192 (13.5)	
Positive	49.0 (18.8-80.8)		17.0 (9.4-31.2)		0.0 (0.0-3.0)		8/29 (27.6)	

For CD4+, CD8+, and FOXP3+ TIL, *p* values were calculated by Mann-Whitney U test, and data are presented as median (interquartile range).

For PD-L1+ immune cell (IC), *p*-values were calculated by chi-square or Fisher's exact test, and data are presented as frequency (%).

3.1.2. Comparison of immune cell subsets between pure DCIS and invasive carcinoma

Next, the difference in immune cell subset infiltration between pure DCIS and invasive carcinoma was examined (**Table 3 & 4**). When comparing pure DCIS and invasive carcinoma in the whole group, infiltration of CD4+, CD8+, and FOXP3+ TILs and the presence of PD-L1+ immune cells were significantly higher in invasive carcinoma compared to pure DCIS (all $p<0.001$; **Table 3**). In invasive breast cancer, TIL infiltration has been reported to be predominant in hormone receptor (HR)-negative tumors including HER2+ and triple-negative subtypes as opposed to HR-positive tumors [14, 28]. In this study, infiltration of immune cells was higher in HR-negative DCIS compared to HR-positive DCIS; thus, subgroup analyses were performed by HR status. In both HR-positive and HR-negative groups, all TIL subsets infiltration and presence of PD-L1+ immune cells were significantly higher in invasive carcinoma than in pure DCIS (all $p<0.001$) (**Table 3**).

Additionally, the dominance of CD4+ versus CD8+ TILs in pure DCIS and invasive carcinoma was examined (**Table 4**). As a whole, infiltration of CD4+ TILs was higher than CD8+ TILs in pure DCIS ($p<0.001$), whereas the reverse was true in invasive carcinoma with the CD8+ TILs being the dominant subset ($p=0.006$). In HR-positive tumors, while there was a higher infiltration of CD4+ T cells compared to CD8+ T cells in pure DCIS ($p<0.001$), there was no difference in the amount of infiltration between the two TIL subsets in invasive carcinoma ($p=0.580$). HR-negative tumors revealed the same pattern of TIL subset dominance as in the whole group.

Table 3. Comparison of immune cell subset infiltration in pure DCIS and invasive carcinoma

Hormone receptor status	Immune cell subset	Pure DCIS (n=231)	Invasive carcinoma (n=359)	<i>p-value</i>
Total	CD4+ TIL	19.3 (4.0-47.8)	85.5 (41.0-176.5)	<0.001
	CD8+ TIL	12.3 (5.3-25.0)	91.5 (42.0-199.3)	<0.001
	FOXP3+ TIL	0 (0-1.0)	9.0 (4.0-19.0)	<0.001
	PD-L1+ IC	34/221 (15.4)	153/350 (43.7)	<0.001
Positive	CD4+ TIL	17.0 (3.7-43.3)	79.0 (38.3-152.0)	<0.001
	CD8+ TIL	11.7 (5.3-22.0)	68.5 (34.0-139.3)	<0.001
	FOXP3+ TIL	0.0 (0.0-0.0)	6.5 (3.0-16.8)	<0.001
	PD-L1+ IC	26/196 (13.3)	72/242 (29.8)	<0.001
Negative	CD4+ TIL	35.0 (18.0-86.5)	125.0 (48.8-209.3)	<0.001
	CD8+ TIL	22.7 (9.2-48.8)	160.0 (81.8-278.3)	<0.001
	FOXP3+ TIL	1.0 (0.0-5.0)	15.0 (7.0-28.0)	<0.001
	PD-L1+ IC	8/25 (32.0)	81/108 (75.0)	<0.001

For CD4+, CD8+ and FOXP3+ TIL, *p*-values were calculated by Mann-Whitney U test, and data are presented as median (interquartile range).

For PD-L1+ immune cell (IC), *p* values were calculated by chi-square or Fisher's exact test, and data are presented as frequency (%).

Table 4. Comparison of CD4+ and CD8+ tumor infiltrating lymphocyte infiltration in individual tumors

Disease group	Hormone receptor status	CD4+TIL >CD8+TIL	CD4+TIL <CD8+TIL	CD4+TIL =CD8+TIL	<i>p-value</i>
Pure DCIS	Total (n=224)	135 (60.3)	88 (39.3)	1 (0.4)	<0.001
	Positive (n=196)	116 (59.2)	79 (40.3)	1 (0.5)	<0.001
	Negative (n=28)	19 (67.9)	9 (32.1)	0 (0.0)	0.016
Invasive carcinoma	Total (n=358)	150 (41.9)	208 (58.1)	0 (0.0)	0.006
	Positive (n=248)	115 (46.4)	133 (53.6)	0 (0.0)	0.580
	Negative (n=110)	35 (31.8)	75 (68.2)	0 (0.0)	<0.001

P-values were calculated by Wilcoxon signed rank test. Data are presented as number of cases (%).

3.1.3. Comparison of immune cell subset infiltration in DCIS and invasive components in a tumor

In order to evaluate the difference in TIL subset infiltration and presence of PD-L1+ immune cells between in situ and invasive components within individual tumors, their infiltration was compared in matched in situ and invasive components using 90 cases of invasive carcinoma with a DCIS component (**Table 5; Figure 2**).

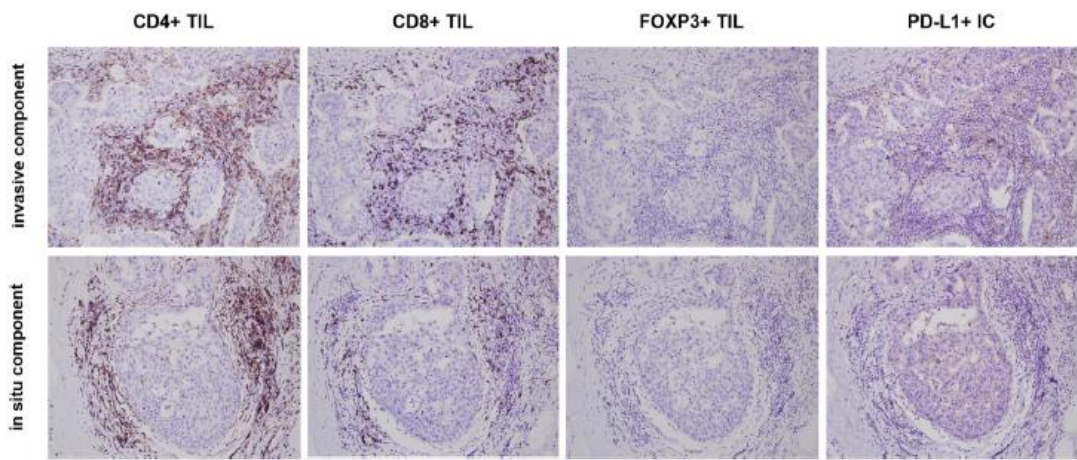


Figure 2. Representative example of CD4+, CD8+, FOXP3+ tumor-infiltrating lymphocytes (TILs) and PD-L1+ immune cell (IC) infiltration in in situ and invasive components in a hormone receptor-negative tumor. CD8+ TIL and PD-L1+ IC infiltration is significantly higher in the invasive component compared to the in situ component while CD4+ TIL infiltration is high in both components with no significant difference. FOXP3+ TILs are rarely found in both invasive and in situ components in this case

All TIL subsets infiltration and the presence of PD-L1+ immune cells were significantly higher in the invasive component compared to the in situ component (all $p<0.001$). HR-positive group revealed a similar pattern as the whole group with significant differences in the number of CD4+, CD8+, and FOXP3+ TILs, and presence of PD-L1+ immune cells between invasive and in situ components ($p<0.001$, $p<0.001$, $p<0.001$, and $p=0.002$, respectively). In HR-negative group, CD8+ and FOXP3+ TILs, and PD-L1+ immune cells were higher in the invasive component compared to the in situ component ($p=0.004$, $p=0.022$, and $p=0.031$, respectively). However, there was no difference in CD4+ TIL infiltration between the two components ($p=0.584$).

Table 5. Comparison of immune cell infiltration in the DCIS and invasive components of individual tumors

Hormone receptor status	Immune cell subset	Invasive component	DCIS component	Invasive >DCIS No. of cases	Invasive<DCIS No. of cases	Invasive=DCIS No. of cases	<i>p-value</i>
All (n=90)	CD4+ TIL	79.5 (42.0-198.5)	38.5 (12.0-101.8)	64	26	0	<0.001
	CD8+ TIL	58.5 (26.8-144.3)	18.0 (5.5-44.3)	71	18	1	<0.001
	FOXP3+ TIL	4.0 (1.0-12.3)	1.0 (0.0-3.3)	56	16	18	<0.001
	PD-L1+ IC	35 (38.9)	19 (21.1)	16 ^a	0 ^b	19 ^c /55 ^d	<0.001
Positive (n=67)	CD4+ TIL	73.0 (26.0-195.0)	18.0 (10.0-65.0)	49	18	0	<0.001
	CD8+ TIL	45.0 (20.0-100.0)	11.0 (3.0-33.0)	53	13	1	<0.001
	FOXP3+ TIL	2.0 (0.0-8.0)	1.0 (0.1-2.0)	41	8	18	<0.001
	PD-L1+ IC	19 (28.4)	9 (13.4)	10 ^a	0 ^b	9 ^c /48 ^d	0.002
Negative (n=23)	CD4+ TIL	124.0 (70.0-220.0)	101.0 (53.0-185.0)	15	8	0	0.584
	CD8+ TIL	143.0 (84.0-274.0)	45.0 (23.0-81.0)	18	5	0	0.004
	FOXP3+ TIL	10.0 (2.0-13.0)	4.0 (1.0-6.0)	15	8	0	0.022
	PD-L1+ IC	16 (69.6)	10 (43.5)	6 ^a	0 ^b	10 ^c /7 ^d	0.031

P-values were calculated by Wilcoxon signed rank test or McNemar test.

Data are presented as median (interquartile range) for CD4+, CD8+ and FOXP3+ TIL and as number of positive cases (%) for PD-L1 immune cell (IC).

a, Invasive (+)/DCIS (-); b, Invasive (-)/DCIS (+); c, Invasive (+)/DCIS (+); d, Invasive (-)/DCIS (-)

3.1.4. Comparison of immune cell subset infiltration in pure DCIS and DCIS-INV

In the next step, the difference in infiltration of TIL subsets and PD-L1+ immune cells between pure DCIS, DCIS-M, and DCIS-INV was determined (**Table 6**). When comparing pure DCIS and DCIS-M in the whole group, infiltration of CD4+ and FOXP3+ TIL was significantly higher in DCIS-M than in pure DCIS (all $p < 0.001$). Comparison of pure DCIS and DCIS-INV revealed higher CD4+ and FOXP3+ TIL infiltrations in DCIS-INV than in pure DCIS ($p = 0.004$, $p = 0.005$, respectively). As a whole, DCIS-M and DCIS-INV revealed no difference in immune cell infiltration.

In HR-positive tumors, FOXP3+ TIL infiltration was significantly higher in DCIS-INV than in pure DCIS ($p < 0.001$) and CD4+ TIL infiltration tended to be higher in DCIS-INV than in pure DCIS ($p = 0.051$). In HR-negative tumors, CD4+ TIL showed a gradual increase from pure DCIS to DCIS-M and DCIS-INV ($p = 0.036$, pure DCIS vs. DCIS-M; $p = 0.063$, DCIS-M vs. DCIS-INV; $p = 0.003$, pure DCIS vs. DCIS-INV). CD8+ TIL infiltration was significantly higher in DCIS-INV compared to pure DCIS and DCIS-M ($p = 0.009$, $p = 0.027$, respectively).

PD-L1+ immune cell infiltration revealed no difference between pure DCIS, DCIS-M, and DCIS-INV regardless of HR status.

Table 6. Comparison of infiltration of immune cell subsets in pure DCIS, DCIS with microinvasion, and DCIS associated with invasive carcinoma

Hormone receptor status	Subset of immune cells	Pure DCIS (n=231)	DCIS-M (n=81)	DCIS-INV (n=90)	<i>p-value</i>			
					<i>Three groups*</i>	<i>Pure DCIS vs. DCIS-M[#]</i>	<i>Pure DCIS vs. DCIS-INV[#]</i>	<i>DCIS-M vs. DCIS-INV[#]</i>
All (n=402)	CD4+ TIL	19.3 (4.0-47.8)	46.3 (16.7-112.1)	38.5 (12.0-101.8)	<0.001	<0.001	<0.001	1.000
	CD8+ TIL	12.3 (5.3-25.0)	18.7 (6.3-47.8)	18.0 (5.5-44.3)	0.027	0.057	0.168	1.000
	FOXP3+ TIL	0 (0-1.0)	1.5 (0.0-10.0)	1.0 (0.0-3.3)	<0.001	<0.001	<0.001	1.000
	PD-L1+ IC	34/221 (15.4)	20/78 (25.6)	19/90 (21.1)	0.111	0.129	0.669	1.000
Positive (n=311)	CD4+ TIL	17.0 (3.7-43.3)	18.3 (6.7-85.7)	18.0 (10.0-65.0)	0.040	0.606	0.051	1.000
	CD8+ TIL	11.7 (5.3-22.0)	15.3 (5.2-34.7)	11.0 (3.0-33.0)	0.684	1.000	1.000	1.000
	FOXP3+ TIL	0.0 (0.0-0.0)	0.0 (0.0-2.0)	1.0 (0.1-2.0)	<0.001	0.225	<0.001	0.573
	PD-L1+ IC	26/196 (13.3)	6/38 (15.8)	9/67 (13.4)	0.916	1.000	1.000	1.000
Negative (n=91)	CD4+ TIL	35.0 (18.0-86.5)	63.3 (31.7-115.0)	101.0 (53.0-185.0)	0.001	0.036	0.003	0.063
	CD8+ TIL	22.7 (9.2-48.8)	25.7 (9.0-64.0)	45.0 (23.0-81.0)	0.007	1.000	0.009	0.027
	FOXP3+ TIL	1.0 (0.0-5.0)	4.0 (1.0-12.0)	4.0 (1.0-6.0)	0.076	0.114	0.159	1.000
	PD-L1+ IC	8/25 (32.0)	14/40 (35.0)	10/23 (43.5)	0.690	1.000	1.000	1.000

*For comparison of three groups, Kruskal-Wallis test or chi-square test were used.

[#] For comparison of two groups, Mann-Whitney U test or chi-square test were used. Corrections for multiple testing are performed with Bonferroni method and adjusted (adj.) *p*-values are presented.

Data are presented as median (interquartile range) for CD4+, CD8+, and FOXP3+ TIL, and as frequency (%) for PD-L1+ immune cell (IC).

3.1.5. Association of immune cell subset infiltration and patient outcome in pure DCIS

Finally, the clinical outcome of the patients with pure DCIS was evaluated in relation to immune cell subset infiltration. Most patients were treated according to standard guidelines and had been followed regularly after surgery. The median follow-up period was 4.7 years (range 0.1-11.5 years) during which 6 patients developed ipsilateral breast recurrence. Recurred tumors were pure DCIS in four patients and invasive ductal carcinoma in the remaining two patients. None of them had metastasis or cancer-related death thereafter. Other clinicopathologic characteristics of these 6 cases are summarized in **Supplementary Table S2**. In survival analyses, none of the clinicopathologic features (extent of DCIS, nuclear grade, comedo-type necrosis, HR status, HER2 status, Ki-67 index, p53 overexpression and margin status) and therapies (type of surgery, adjuvant radiation therapy and adjuvant endocrine therapy) were associated with ipsilateral breast recurrence. As for immune cell subset infiltration, high infiltration of FOXP⁺ TILs and presence of PD-L1⁺ immune cells were found to be associated with decreased recurrence-free survival ($p=0.002$, $p=0.018$, respectively; **Figure 3**).

However, CD4⁺ and CD8⁺ TIL infiltration did not show prognostic significance ($p=0.287$, $p=0.445$, respectively, log rank test). As the infiltration of TIL subsets was correlated with one another, we also analyzed the relationship between the ratios of TIL (FOXP3⁺/CD8⁺ TIL, FOXP3⁺/CD4⁺ TIL and CD4⁺/CD8⁺ TIL) and tumor recurrence. High FOXP3⁺/CD8⁺ TIL ratio and high FOXP3⁺/CD4⁺ TIL ratio were associated with decreased recurrence-free survival ($p=0.023$, $p=0.036$, respectively; **Figure 3**)

Of the 6 cases with ipsilateral breast recurrence, 5 cases were HR-positive. In subgroup analyses of HR-positive pure DCIS, high infiltration of FOXP3+ TILs and presence of PD-L1+ immune cells also revealed association with decreased recurrence-free survival ($p=0.019$, $p=0.002$, respectively).

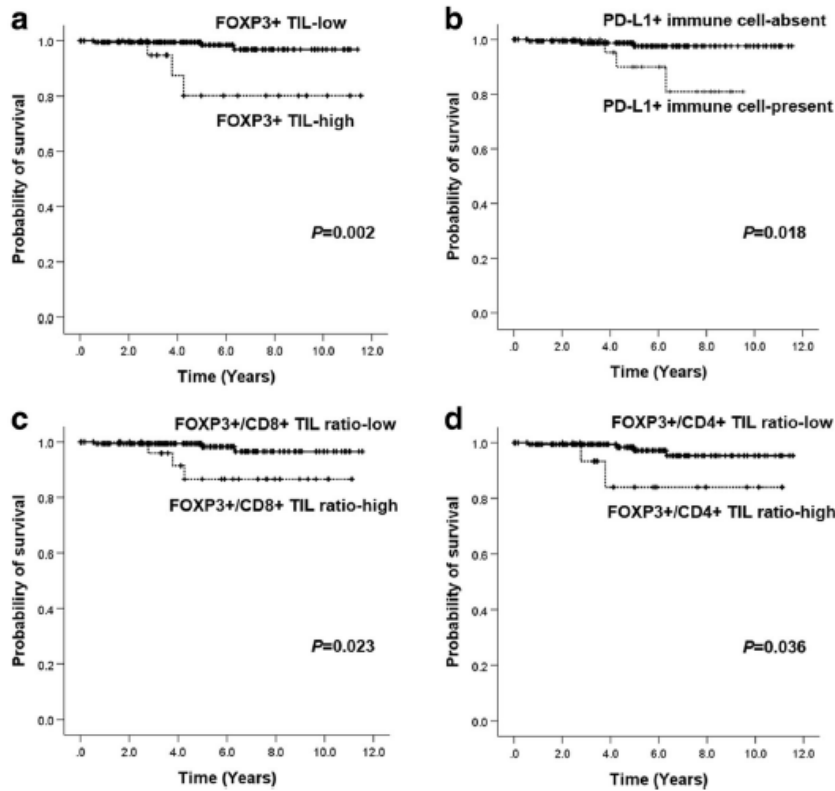


Figure 3. Kaplan-Meier survival curves stratified by immune cell subset infiltration and their ratio in pure DCIS. High level of FOXP3+ tumor-infiltrating lymphocyte (TIL) infiltration (a), the presence of PD-L1+ immune cells (b), high FOXP3+/CD8+ TIL ratio (c), and high FOXP3+/CD4+ TIL ratio (d) are associated with decreased recurrence-free survival.

3.2. Immune-related gene expression in DCIS and invasive carcinoma

Since the immune cell infiltration in all TIL subsets and PD-L1+ immune cells were generally greater in invasive carcinoma compared to pure DCIS and DCIS-M, it was hypothesized that there must be immunologic difference between DCIS and invasive carcinoma which affects their tumor microenvironment. Thus, using 770 immune-related gene panel, the difference in immune-related gene expression was evaluated in DCIS and invasive carcinoma. List of top 20 immune related genes with significant difference between DCIS and invasive carcinoma are summarized in **Table 7**. Among top 20 genes, those with Log2 fold change greater than 1.5 with adjusted *p*-value less than 0.05 were CXCL10 and CXCL9. Especially, CXCL10 had the greatest fold change with Log2 fold change value of 2.92 with adjusted *p*-value of 0.00313.

In ER-positive subgroup, of 28 cases analyzed, none of the genes revealed significant difference between DCIS and invasive carcinoma. However, S100A8, LAG3, CXCL10 and CXCL9 had difference in fold change between DCIS and invasive carcinoma, although statistically not significant (adjusted *p*-value>0.05; **Supplementary Table S5**). In ER-negative subgroup, no genes were significantly different between DCIS and invasive carcinoma. CXCL10 had a largest fold change value of 3.44 but with *p*>0.05. The list of top 20 genes with difference in fold change between DCIS and invasive carcinoma in ER-negative subgroup are summarized in **Supplementary Table S6**.

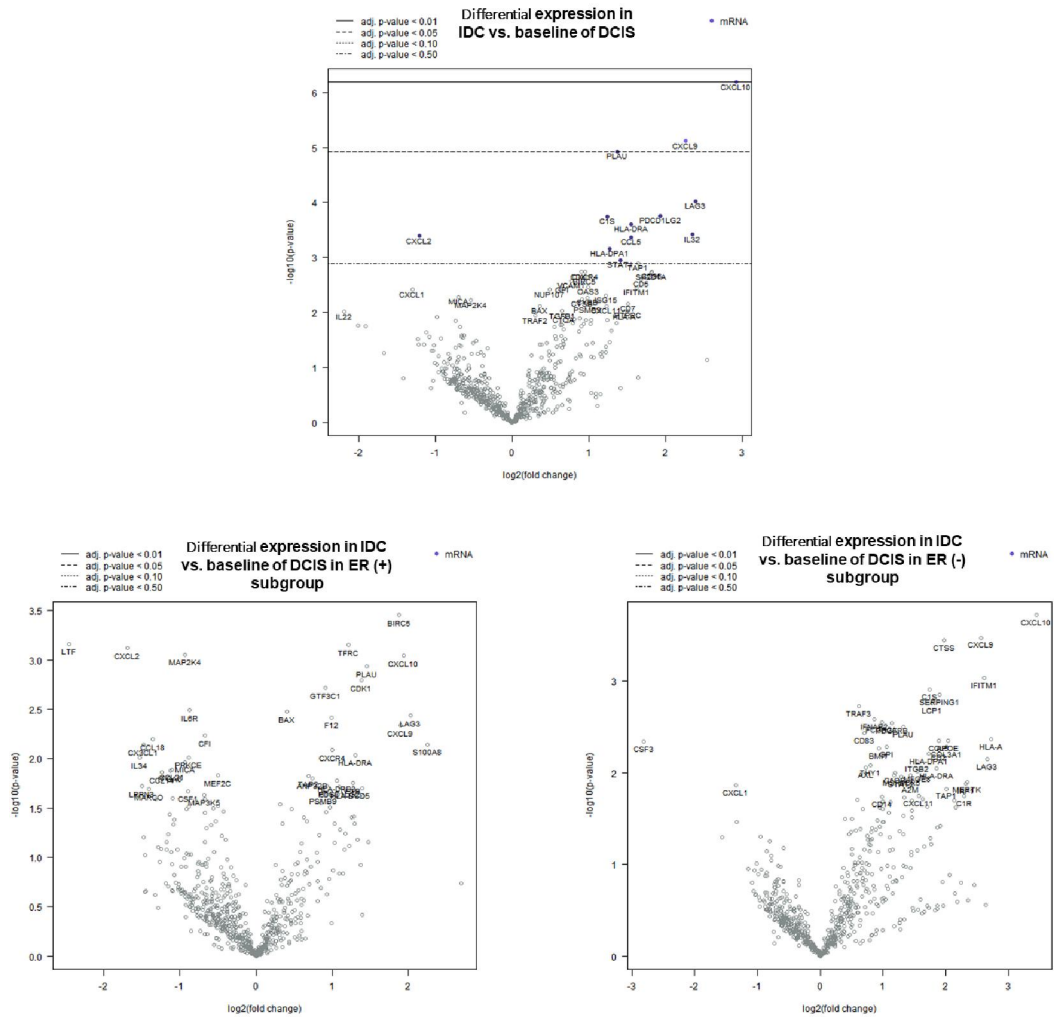


Figure 4. Volcano plot shows differential expression of invasive carcinoma compared to base line DCIS in the whole group, ER + subgroup and ER- subgroup. In the whole group, CXCL10 and CXCL9 showed fold change 2.92 and 2.26, with adjusted p -value <0.05. In ER-positive group, there was no significant difference between invasive carcinoma and DCIS in immune-related gene expression with all adjusted p -value >0.05. In ER-negative subgroup, although statistically not significant, CXCL10 and CXCL9 had tendency to be increased in invasive carcinoma with fold change 3.44 and 2.56.

Table 7. List of top 20 genes with significant fold change between DCIS and invasive carcinoma

Gene (mRNA)	Log2 fold change	P-value	Adjusted p-value[#]
CXCL10	2.92	6.50E-07	0.00313
LAG3	2.39	9.43E-05	0.114
IL32	2.35	0.000385	0.206
CXCL9	2.26	7.67E-06	0.0185
PDCD1LG2	1.93	0.000175	0.145
CD96	1.82	0.00182	0.532
SH2D1A	1.81	0.00187	0.532
CD5	1.68	0.00249	0.631
TAP1	1.64	0.00128	0.476
HLA-DRA	1.55	0.000251	0.173
CCL5	1.55	0.000428	0.206
STAT1	1.41	0.00113	0.452
PLAU	1.37	1.18E-05	0.0189
HLA-DPA1	1.27	0.000696	0.305
C1S	1.24	0.000181	0.145
CXCR4	0.952	0.00184	0.532
BIRC5	0.947	0.00226	0.605
CK1	0.9	0.00184	0.532
VCAM1	0.775	0.00266	0.64
CXCL2	-1.21	0.000407	0.206

DCIS includes pure DCIS and DCIS with microinvasion

[#] *p*-values adjusted by Benjamini-Yekutieli procedure

3.3. Validation of a selected gene, CXCL10 in DCIS and invasive carcinoma

3.3.1. Comparison of CXCL10 mRNA expression in DCIS and invasive carcinoma

Difference in CXCL10 mRNA expression was examined between DCIS and invasive carcinoma in the whole groups, in HR-positive subgroup, as well as in HR-negative subgroup (**Table 8**). In the whole group, expression of CXCL10 mRNA, evaluated by the fold change ($2^{-\Delta\Delta\text{ct}}$), was significantly higher in invasive carcinoma than in DCIS ($p < 0.001$). However, in HR-positive subgroup, CXCL10 mRNA expression was not significantly different between the two groups ($p = 0.260$). In the HR-negative subgroup, CXCL10 mRNA expression was significantly higher in invasive carcinomas compared to DCIS ($p < 0.001$), similar to the whole group.

3.3.2. Comparison of CXCL10 expression between DCIS and DCIS-INV

The difference in CXCL10 mRNA expression between DCIS and DCIS-INV was also examined. CXCL10 mRNA expression was significantly higher in DCIS-INV than in DCIS in the whole group and in HR-negative subgroup ($p = 0.011$ and $p = 0.020$, respectively). In HR-positive subgroup, there was no significant difference in CXCL10 mRNA expression between the two groups. The results are summarized in **Table 9**.

Table 8. Comparison of CXCL10 mRNA expression between DCIS and invasive carcinoma

Hormone receptor status	DCIS*	Invasive carcinoma	<i>p</i> value
Total	57.41 (0.73-283.99)	332.37 (147.96-518.05)	<0.001
Positive	158.48 (0.44-453.45)	291.92 (176.96-577.25)	0.260
Negative	6.82 (1.02-233.83)	402.28 (102.49-507.57)	<0.001

p-values were calculated by Mann-Whitney U test, and data are presented as median (interquartile range)

*DCIS includes pure DCIS and DCIS with microinvasion

Table 9. Comparison of CXCL10 mRNA expression between DCIS and DCIS associated with invasive carcinoma

Hormone receptor status	DCIS*	DCIS associated with invasive carcinoma	<i>p</i> value
Total	57.41 (0.73-283.99)	215.82 (76.31-417.18)	0.011
Positive	158.48 (0.44-453.45)	215.82 (68.26-417.18)	0.301
Negative	6.82 (1.02-233.83)	180.13 (76.74-772.92)	0.020

p-values were calculated by Mann-Whitney U test, and data are presented as median (interquartile range)

*DCIS includes pure DCIS and DCIS with microinvasion

3.3.3. Comparison of CXCL10 mRNA expression in DCIS and invasive components within a same tumor

CXCL10 mRNA expression was also evaluated in invasive and DCIS components within a same tumor. As a whole, invasive component of tumor generally showed higher level of CXCL10 mRNA expression compared to DCIS component. However, CXCL10 mRNA expression was not significantly different between DCIS and invasive components of the same tumor in all group, HR-positive and HR-negative subgroups ($p=0.710$, $p=0.754$ and $p=0.875$, respectively; **Table 10**).

Table 10. Comparison of CXCL10 mRNA expression in DCIS and invasive components of individual tumors

Hormone receptor status	DCIS component	Invasive component	Invasive<DCIS No. of cases	Invasive>DCIS No. of cases	Invasive=DCIS No. of cases	<i>p-value</i>
All (n=24)	215.82 (76.31-417.18)	407.10 (80.63-691.45)	12	12	0	0.710
Positive (n=12)	215.82 (68.26-417.18)	479.59 (120.94-761.54)	6	6	0	0.754
Negative (n=12)	180.14 (76.74-772.92)	313.63 (52.96-611.03)	6	6	0	0.875

P-values were calculated by Wilcoxon signed rank test.

Data are presented as median (interquartile range)

3.3.4. Correlation of CXCL10 mRNA expression with TIL infiltration in DCIS and invasive carcinoma

Since CXCL10 is a chemokine that is known to attribute to chemoattraction of inflammatory cells including T cells, the correlation between CXCL10 expression and TIL density was evaluated. In DCIS, CXCL10 mRNA and TIL infiltration showed a weak positive correlation ($\rho=0.270$, $p=0.037$). In invasive carcinoma, CXCL10 mRNA expression also showed weak positive correlation with TIL density ($\rho=0.382$, $p=0.003$) (**Figure 5**).

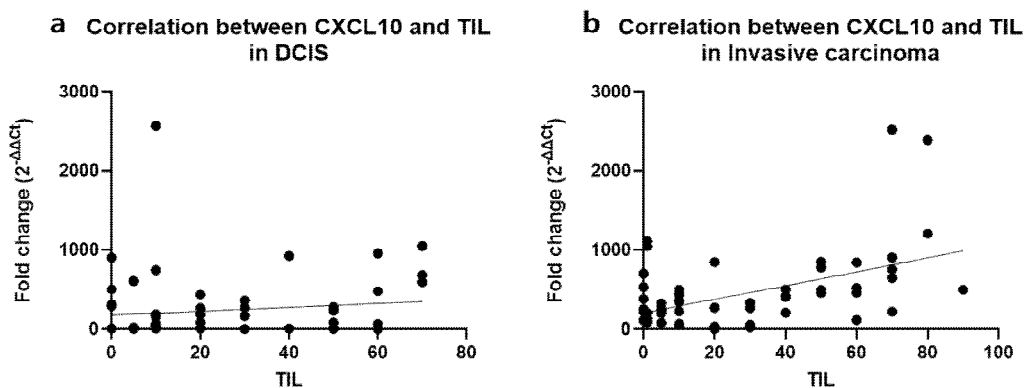
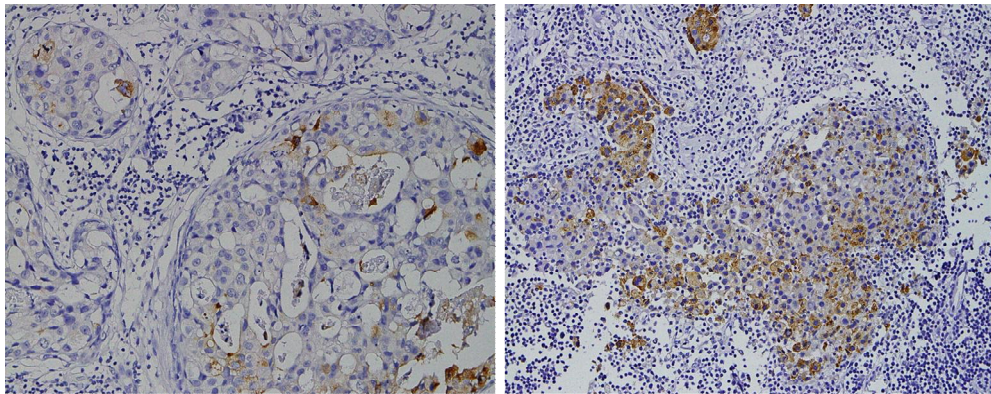


Figure 5. Correlation between tumor infiltrating lymphocytes (TILs) and CXCL10 mRNA fold change ($2^{-\Delta\Delta Ct}$) in DCIS (**a**) and invasive carcinoma (**b**). Both showed positive weak correlation, with $\rho=0.270$, and $\rho=0.382$, respectively.

3.4. CXCL10 expression and its association with immune cell subset infiltration in DCIS and invasive carcinoma

3.4.1. CXCL10 expression and its relationship with clinicopathologic features of tumor

In DCIS, CXCL10 expression detected by immunohistochemistry was not frequent, but staining pattern was similar to that of invasive carcinoma with dot-like cytoplasmic or membranous staining in both tumor cells and peri-tumoral stromal area (**Figure 6**). Of 223 cases of DCIS, CXCL10 expression was observed in 21 cases (9.4%). In invasive carcinoma, CXCL10 was more commonly observed compared to DCIS with 81 cases (21.8%) of CXCL10 positive tumors among 372 cases of invasive carcinomas. Expression of CXCL10 was mainly found in tumor cells although some tumor stromal cells also showed positive staining pattern (**Figure 6**).



Ductal carcinoma in situ

Invasive carcinoma

Figure 6. Representative images of CXCL10 expression in DCIS and invasive carcinoma using immunohistochemistry. Membranous or cytoplasmic staining in tumor cells as well as stromal cells in tumor area with dot-like staining pattern were considered positive expression. In general, cases with CXCL10 expression often had increased tumor infiltrating lymphocyte infiltration, as shown in the above image.

In the whole group and in HR-negative subgroup, CXCL10 expression was significantly higher in invasive carcinoma than in DCIS ($p<0.001$). However, there was no difference between the two groups in HR-positive subgroup (**Figure 7**).

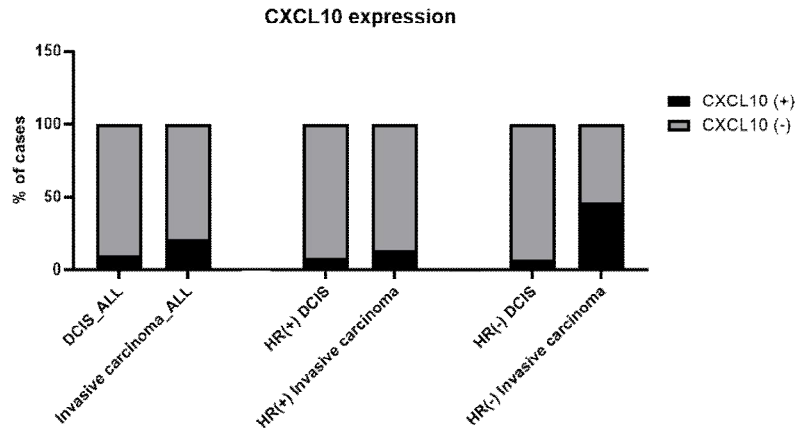


Figure 7. Comparison of CXCL10 expression between DCIS and invasive carcinoma. In the whole group and in hormone receptor-negative subgroup, expression of CXCL10 was significantly higher in invasive carcinoma than in DCIS ($p<0.001$). However, there was no significant difference between DCIS and invasive carcinoma in hormone receptor-positive subgroup.

None of the clinicopathologic features were associated with CXCL10 in DCIS (**Supplementary Table S11**). However, in invasive carcinoma, high histologic grade, ER negativity, PR negativity, high Ki-67 proliferation index and p53 overexpression and triple negative subtype were associated with CXCL10 expression (all $p<0.005$) (**Supplementary Table S12**).

3.4.2. Correlation of immune cell subset infiltration with CXCL10 expression

CXCL10 expression was correlated with CD4+, CD8+, FOXP3+ TILs and PD-L1+ immune cell infiltration in DCIS (**Table 11**). In the whole group, CD4+, CD8+, FOXP3+ TIL and PD-L1+ immune cell infiltration was significantly higher in CXCL10-positive groups than in CXCL10-negative group ($p=0.001$, $p=0.001$, $p<0.001$ and $p<0.001$, respectively).

In HR-positive subgroup, similar to the whole group, CD4+, CD8+, FOXP3+ TIL and PD-L1+ immune cell infiltration was greater in CXCL10-positive tumors (all $p<0.05$). In HR-negative subgroup, only FOXP3+ TIL showed significant difference between CXCL10-positive and negative groups ($p=0.001$). CD4+ and CD8+ TIL tended to be higher in CXCL10-positive tumors. Although number of cases are limited, PD-L1+ immune cell infiltration also tended to be higher in CXCL10+ tumors.

In invasive carcinoma (**Table 11**), CD8+ and FOXP3+ TIL infiltration as well as PD-L1+ immune cell infiltration was higher in CXCL10-positive tumors ($p=0.007$, $p=0.001$, and $p=0.001$, respectively). In HR-positive invasive tumors, there was no significant difference in CD4+, CD8+, FOXP3+TIL and PD-L1+ immune cell infiltration according to CXCL10 expression. In HR-negative tumors, FOXP3+TIL and PD-L1+ immune cell infiltration was also significantly higher in CXCL10-positive tumors than in CXCL10-negative tumors ($p=0.019$ and $p=0.002$, respectively).

Table 11. Comparison of immune cell subset infiltration in relation to CXCL10 expression in DCIS and invasive carcinoma

Immune cell subset	DCIS*		<i>p</i> value	Invasive carcinoma		<i>p</i> value
	CXCL10 (+)	CXCL10 (-)		CXCL10 (+)	CXCL10 (-)	
Total						
CD4+ TIL	77.33 (23.50-116.67)	25.1 (7.00-52.75)	0.001	72.50 (35.25-155.50)	88.00 (47.00-186.00)	0.507
CD8+ TIL	36.33 (16.33-66.83)	12.33 (5.50-25.67)	0.001	120.00 (56.75-249.00)	65.00 (32.50-142.00)	0.008
FOXP3+ TIL	4.67 (0.00-12.83)	0.00 (0.00-2.00)	<0.001	13.00 (5.00-21.00)	5.00 (2.00-12.50)	0.001
PD-L1+ IC	11/21 (52.4)	34/200 (17.0)	<0.001	24/36 (66.7)	40/113 (35.4)	0.001
HR+ subgroup						
CD4+ TIL	58.83 (21.42 -104.58)	18.00 (5.00-47.08)	0.004	91.00 (38.75-160.25)	88.00 (49.00-172.00)	0.890
CD8+ TIL	31.67 (13.91-52.08)	11.33 (5.00-22.00)	0.006	70.00 (56.00-206.00)	58.00 (30.00-130.00)	0.120
FOXP3+ TIL	0.50 (0.00-5.33)	0.00 (0.00-0.00)	0.024	7.00 (3.50-18.50)	5.00 (2.00-11.00)	0.179
PD-L1+ IC	6/14 (42.9)	20/156 (12.8)	0.009	7/18 (38.9)	29/62 (31.9)	0.563
HR- subgroup						
CD4+ TIL	109.33 (23.33-126.00)	50.17 (24.58-96.33)	0.175	70.00 (33.75-157.00)	106.00 (32.25-228.75)	0.563
CD8+ TIL	49.0 (31.00-76.33)	20.17 (8.25-51.75)	0.124	133.50 (89.00-322.50)	109.00 (36.00-262.00)	0.262
FOXP3+ TIL	15.00 (8.00-17.33)	2.50 (0.00-7.75)	0.001	16.50 (10.75-31.50)	8.00 (3.75-15.00)	0.019
PD-L1+ IC	5/7 (71.4)	14/44 (31.8)	0.087	17/18 (94.4)	11/22 (50.0)	0.002

P values are calculated by Mann-Whitney U test. Data are presented as median (interquartile range) for TIL and frequency (%) for PD-L1+ immune cell (IC).

*DCIS includes pure DCIS and DCIS with microinvasion

4. Discussion

In this study, high infiltration of CD4+, CD8+, and FOXP3+ T cells and the presence of PD-L1+ immune cells were generally associated with aggressive features of DCIS including high nuclear grade, comedo-type necrosis, HR-negativity, and high Ki-67 proliferation index. Increased TIL density in DCIS has been associated with high-risk features including large tumor size, high nuclear grade, comedo-type necrosis, ER-negativity, and HER2-positivity in previous studies [15, 16, 29]. As TIL subset infiltration is higher in TIL-rich DCIS, it is reasonable to assume that high TIL subset infiltration is associated with aggressive features of DCIS. As for the relationship between TIL subset infiltration and characteristics of DCIS, a few studies have reported a positive correlation between TIL subset infiltration such as CD4+, CD8+, FOXP3+, and CD20+ T cells and nuclear grade of DCIS [17, 30]. Similarly, the presence of PD-L1+ immune cells in DCIS has been reported to be associated with high TIL infiltration, younger patient age, ER-negativity, and HER2-positivity in previous studies [16, 20-22].

Dense TIL infiltration in DCIS has been linked to a high risk of progression [15, 16]. As for the composition of TILs, low CD8+ T cells, low CD8+/FOXP3+ ratio, and low CD8+HLA-DR+ cells have been reported to be associated with ipsilateral recurrence [17, 19]; high numbers of B cells were associated with shorter recurrence-free interval in DCIS [18]. In this study, high infiltration of FOXP3+ TIL, high FOXP3+/CD8+ TIL ratio, and high FOXP3+/CD4+ TIL ratio were associated with decreased recurrence-free survival. Moreover, the presence of PD-L1+ immune cell was associated with poor recurrence-free survival. These results suggest that suppression of anti-tumor immunity by FOXP3+ TILs and PD-

L1+ immune cells play an important role during progression of DCIS. Thus, pure DCIS with high FOXP3+ TIL infiltration or PD-L1+ immune cells could be a target for active surveillance or aggressive treatment. However, the analyses about tumor recurrence have a limitation in that only a small number (n=6) of cases revealed ipsilateral breast recurrence. Moreover, clinicopathologic variables which were known to be associated with recurrence in pure DCIS were not associated with tumor recurrence in this study. Thus, the results should be interpreted cautiously and further large studies are warranted to confirm these findings.

Evaluation of difference in immune cell infiltration between DCIS and invasive carcinoma, and also among pure DCIS, DCIS-M, and DCIS-INV may provide some insight into its role during DCIS progression. All TIL subsets infiltration and the presence of PD-L1+immune cells were higher in invasive carcinoma than in pure DCIS irrespective of HR status as in previous studies which reported a gradual increase in the number of immune cells during progression of breast cancer [31, 32]. Interestingly, in this study, HR-negative breast cancers revealed high CD4+ TIL infiltration in both in situ and invasive components of the same tumors with no statistical difference. Moreover, in HR-negative tumors, CD4+ TIL showed a gradual increase from pure DCIS to DCIS-M and DCIS-INV. These findings suggest that CD4+ T cells increase at an early stage of DCIS progression in HR-negative tumors and may play a crucial role during in situ to invasive transition in HR-negative tumors. However, CD4+ TILs by subsets were not evaluated except for FOXP3+ regulatory T cells. Infiltration of FOXP3+ TILs did not differ between pure DCIS, DCIS-M, and DCIS-INV in HR-negative group. It is well known that CD4+ TILs display a large degree of plasticity and the ability to differentiate into multiple sublineages in response to environmental cues [33].

CD4⁺ Th1 cells, CD4⁺ CTLs, and follicular helper T cells exert potent antitumor activity, whereas regulatory T cells or, under certain circumstances, CD4⁺ Th2 cells and CD4⁺ Th17 cells show tumor-promoting activity [33, 34]. Thus, in further studies, analyses of CD4⁺ TIL subsets would be crucial to find the overall effect of heavy CD4⁺TIL infiltration around HR-negative DCIS.

In HR-positive breast cancers, despite the fact that FOXP3⁺ TIL was significantly higher in DCIS-INV than pure DCIS, the other TIL subsets seemed to increase in number at a late stage of DCIS progression, or seemed unlikely to be associated with in situ to invasive transition. Growing evidence supports a role of host immune surveillance in influencing response to therapy and prognosis in HER2⁺ and triple-negative breast cancer, but not in HR-positive breast cancer which appears to be less immunogenic than HER2⁺ and triple-negative breast cancer [7]. However, it has been reported that FOXP3⁺ TIL infiltration is strongly associated with adverse clinical outcome in HR-positive breast cancer [14, 35, 36]. Furthermore, in the present study, infiltration of FOXP3⁺TIL was associated with tumor recurrence in HR-positive pure DCIS. Thus, treatment or prevention of tumor progression in HR-positive breast cancer would have to be focused on FOXP3⁺ regulatory T cells.

The mechanism by which immune cells influence tumor cell invasion in DCIS is unclear. Degradation of the basement membrane, a prerequisite for tumor invasion, has been attributed primarily to over-production of proteolytic enzymes by the tumor or the surrounding stromal cells [37]. However, cumulating data support a hypothesis that myoepithelial cells act as “natural tumor suppressors” and lose such property during tumor progression [38]. Man et al. reported that leukocyte infiltration was increased at focal myoepithelial cell disruption sites in

DCIS, suggesting that a localized death of myoepithelial cells and subsequent immune reactions are a trigger for myoepithelial cell layer disruptions, basement membrane degradation, and tumor invasion [39]. Conversely, it can be postulated that when tumor cells with an increased invasive property invade the stroma, it activates the immune system leading to more immune cell infiltration around DCIS with invasion.

In this study, CD4⁺ and FOXP3⁺ TIL infiltration was significantly higher in DCIS-M and DCIS-INV compared to pure DCIS in the whole group. CD4⁺ and CD8⁺ TIL infiltration was significantly higher in DCIS-INV than in pure DCIS in HR-negative group, and FOXP3⁺ TIL infiltration was significantly higher in DCIS-INV than in pure DCIS in HR-positive group. Beguinot et al. reported that microinvasive carcinoma showed a significantly higher TIL density with more CD8⁺, CD4⁺, and CD38⁺ cell infiltration than pure DCIS. Toss et al. also showed that DCIS-INV showed denser TILs as opposed to pure DCIS [15]. Although these authors did not show the difference in TIL infiltration according to HR status, their findings are consistent with the results of this study. It is known that in situ and invasive components of the same tumor exhibit similar patterns of genetic alterations [40]. Thus, tumor cells in DCIS-INV may show higher immunogenicity than tumor cells in pure DCIS eliciting stronger immune responses compared to pure DCIS.

From the findings on the difference in TIL subset and PD-L1⁺ immune cell infiltration between DCIS and invasive carcinoma, the difference in terms of immune related gene expression between the two disease groups was analyzed using Nanostring nCounter platform. Even though the cases were limited, the immune related gene that showed the most striking difference between the two

groups was CXCL10. Therefore, using CXCL10 as a target molecule, its expression was analyzed in DCIS and invasive carcinoma in relation to immune cell subset infiltration.

Recent studies focused on the role of CXCL9, CXCL10, CXCL11/CXCR3 axis as it regulates differentiation of naïve T cells to T helper cells, activates and recruits immune cells, such as CTLs, NK cells, NKT cells and macrophages in response to IFN- γ [24, 25, 41]. CXCL10, which is a ligand of CXCR3, is mainly secreted by monocytes, endothelial cells, fibroblasts and cancer cells [42]. The classic view on CXCL10 considered it to prevent cancer through paracrine signaling as CXCL10 plays an important role in the recruitment and activation of immune cells [43]. However, there is an increasing evidence that the CXCL9, CXCL10, CXCL11/CXCR3 axis plays a tumorigenic role causing tumor progression and metastasis both in vitro as well as in vivo; it is thought to be done by autocrine signaling of cancer cells, which increase cell proliferation, angiogenesis, and metastasis [44-49]. With the role of CXCL10 as a mediator of inflammatory reaction as well as tumorigenesis, a better understanding of the difference of its expression in DCIS and invasive carcinoma is necessary; it will potentially provide in depth knowledge of tumor microenvironment of DCIS.

In present study, CXCL10 expression was significantly higher in invasive carcinoma than in DCIS. In a previous study which evaluated expression of CXCL10 in 6 cases of breast cancer comprised with 3 cases of DCIS and 3 cases of invasive carcinoma compared to normal breast using immunohistochemistry, invasive carcinoma showed markedly increased expression of CXCL10. DCIS also showed increased expression compared to normal breast tissue, but intensity and distribution of staining was less than that of invasive carcinoma [50]. Ejaeidi and

his colleagues showed in their study the elevation of CXCL10 in breast cancer patient's sera compared to healthy controls in a hormone independent manner [48]. Interestingly, in this study, CXCL10 expression was significantly different between DCIS and invasive carcinoma in HR-negative subgroup, but not in HR-positive subgroup. It can be postulated that since CXCL10 expression correlated with high TIL infiltration and HR-negative tumors often have more TILs, the difference in CXCL10 expression may be accentuated between DCIS and invasive carcinoma in HR-negative tumors.

Moreover, CXCL10 expression was significantly increased in DCIS-INV compared to DCIS in the whole group and in HR-negative subgroup and there was no difference in CXCL10 expression in DCIS component and invasive component within the same tumor. Ma et al. suggested in their study that gene expression alteration conferring the potential for invasive growth are already present in preinvasive stage [46]. Having no difference in CXCL10 expression within DCIS and invasive components of the same tumor may represent the early alteration of gene expression. However, this should be further confirmed in larger studies.

In this study, none of the clinicopathologic features were associated with CXCL10 expression in DCIS. However, similar to previous publications [44][51], expression of CXCL10 was associated with high nuclear grade, ER negativity, PR negativity, high ki-67 proliferation index and was mostly upregulated in triple negative subtype in invasive carcinoma.

TIL infiltration had positive correlation with CXCL10 expression both in DCIS and invasive carcinoma in this study. Due to paracrine effect of CXCL10 in immune cell migration, differentiation, and activation, areas with CXCL10 expression would have increased TIL infiltration. In DCIS, all subsets of TIL and

PD-L1+ immune cells infiltration correlated with CXCL10 positivity, while in invasive carcinoma, CD8+ and FOXP3+ TIL, and PD-L1+ immune cell infiltration significantly increased in CXCL10-positive tumors with no significant difference in CD4+ TIL infiltration. CXCR3, which is an inflammatory chemokine receptor of CXCL10, is known to be associated with CD4+ Th1 cells and CD8+ CTLs [52, 53]. These receptors are known to be activated when their ligand CXCL10, CXCL9 and CXCL11 bind to the receptor. However, as shown in this study, the reason why CD4+ TIL infiltration differ in DCIS but not in invasive carcinoma in relation to CXCL10 expression needs more investigations.

FOXP3+ TIL infiltration increased in conjunction with CXCL10 expression. In the study on liver graft injury, post-transplant enhanced CXCL10/CXCR3 signaling induced mobilization and recruitment of Tregs, which further promoted tumor growth and recurrence [54]. In pancreatic ductal adenocarcinoma, CXCL10 has been shown to recruit CD4+, CD8+ and CXCR3+ T cells, as well as FOXP3+ Tregs [55]. There also has been a study that CXCL10 drive increased transcription of T-bet and ROR γ , leading polarization of naïve t cells to FOXP3- type 1 regulatory T cells or T helper 17 cells through STAT1, STAT4, and STAT5 phosphorylation [56]. The detailed function of CXCL10 on FOXP3+ Tregs in breast cancer should be further elucidated, yet it can be concluded from the result that FOXP3+ TIL infiltration is greater in CXCL10 positive tumors in both DCIS and invasive carcinoma.

Increased PD-L1+ immune cells were associated with CXCL10 expression in both DCIS and invasive carcinoma in this study. Peng et al. showed that anti-PD-1 therapy not only reduced size of tumor, but upregulated the expression of CXCL10 in tumor microenvironment through IFN- γ [57]. In gastric cancer, CXCL9,

CXCL10, CXCL11/CXCR3 axis have been suggested to regulate PD-L1 expression through STAT and PI3K-Akt pathway [58]. Another study using CXCR3 knock out mice showed that Anti-PD-1 therapy failed to reduce tumor, suggesting the importance of CXCL9, CXCL10, CXCL11/CXCR3 axis in the effectiveness of PD-L1 therapy [59]. Through these findings, it can be postulated that CXCL10 positivity may be used together with PD-L1 expression to predict anti-PD-1 therapy effect.

In this study, there were more CD4⁺ T cells than CD8⁺ T cells infiltrating pure DCIS regardless of HR status. In invasive carcinoma, CD4⁺ and CD8⁺ T cell infiltration showed no difference in HR-positive tumors, whereas CD8⁺ T cells were predominant in HR-negative tumors. In line with this study, Thompson et al. found slightly more CD4⁺ T cells than CD8⁺ T cells in DCIS [20], and Sheu et al. showed that CD8⁺ T cells significantly increased with stage progression of invasive breast cancer [60]. On the contrary, Gil Del Alcazar et al. [61] reported a decrease in CD8⁺ signatures in invasive breast cancer and fewer activated GZMB⁺CD8⁺ T cells in invasive breast cancer compared to DCIS. However, these studies were conducted using a small series, and we observed a greater infiltration of CD8⁺ T cells than CD4⁺ T cells in a minority of DCIS, and vice versa in some cases of invasive carcinoma. Thus, further large-series studies investigating the composition of TIL subsets in DCIS and their change during tumor progression are required to understand the role of individual TIL subsets during tumor progression.

The current study includes a relatively large number of cases that can provide a general idea on changes in immune cell infiltration during in situ to invasive transition. Moreover, this is the first large study comparing CXCL10 expression in DCIS and invasive carcinoma. However, this study has some limitations. First,

even though the International Immuno-Oncology Biomarker Working Group recently published a proposal for evaluation of TILs on hematoxylin & eosin-stained sections in DCIS [26, 27], the scoring system for TIL subsets by immunohistochemistry in DCIS has not been optimized yet. It is recommended that only stromal TILs be evaluated as mean values in DCIS [26, 27]. However, both intra-tumoral and stromal TIL subsets were evaluated in hot spots of DCIS to compare with the previous study data of TIL subset infiltration in invasive carcinoma even though most of the TIL subsets were found in the stromal compartment. Second, evaluation of immune cell subsets was confined to CD4+, CD8+, FOXP3+ TILs, and PD-L1+ immune cells, and their subtypes or activation status was not assessed. In addition, although TIL subset and PD-L1+ immune cell infiltration in DCIS may be heterogeneous from one area to another, the cells were counted using the TMA platform in order to evaluate a large number of samples which may have resulted in selection bias. Furthermore, the expression of CXCL10 can be best described when explained together with other chemokines in CXCL9, CXCL10, CXCL11, and CXCR3. Especially, CXCR3, which is also known as G protein-coupled receptor 9 (GPCR9) or CD183, has three variants: CXCR3A, CXCR3B and CXCR3-alt. These variants are known to have different function, where CXCR3A can have pro-tumor effect and CXCR3B has anti-tumor effect [62, 63] . Since CXCL10 can have different effect on which receptor they bind to [64], interpretation of CXCL10 expression with CXCR3 may be useful. However, immunohistochemistry cannot differentiate the variants of CXCR3, thus variant-specific expression should further be confirmed using a different modality.

5. Conclusion

In summary, this study showed that immune microenvironment of DCIS is different from that of invasive carcinoma. CD4+, CD8+, and FOXP3+ TIL, and PD-L1+ immune cell infiltration was significantly higher in invasive carcinoma compared to pure DCIS regardless of HR status. In HR-negative tumors, there was no difference in CD4+ TIL infiltration between in situ and invasive components within the same tumors, and it increased in a stepwise fashion from pure DCIS to DCIS-M and DCIS-INV, indicating its possible role during early stage of HR-negative DCIS progression. In HR-positive tumors, all immune cell infiltrations were higher in the invasive component than the DCIS component, and FOXP3+ TIL was significantly higher in DCIS-INV than pure DCIS. High infiltration of FOXP3+ TIL and the presence of PD-L1+ immune cells were associated with tumor recurrence in patients with pure DCIS, suggesting a potential benefit in active surveillance or aggressive treatment in such patient groups. CXCL10 expression was significantly higher in invasive carcinoma than in DCIS in the whole group and HR-negative tumors. CXCL10 expression was also different between DCIS and DCIS-INV, with increased expression of CXCL10 in DCIS-INV in the whole group and HR-negative group. In general, CXCL10 positive tumors showed higher infiltration of CD4+, CD8+ and FOXP3+ TILs and PD-L1+ immune cells. Taken together, CXCL10 seems to lead to the difference in immune cell infiltration between DCIS and invasive carcinoma, suggesting its critical role in tumor immune microenvironment and progression of DCIS. Currently, patients diagnosed with DCIS need to undergo surgical resection as there are no utilized biomarker that predict progression of DCIS to invasive carcinoma. By further

understanding tumor microenvironment associated with progression of DCIS, it may be possible to provide individualized treatment to patients in future.

Supplementary Tables

Supplementary Table S1. Correlations in infiltration of CD4+, CD8+, and FOXP3+ tumor infiltrating lymphocytes and PD-L1+ immune cells (ICs) in pure DCIS

Correlation between markers	CD4+ TIL	CD8+ TIL	FOXP3+ TIL	PD-L1+ IC
CD4+ TIL	-	0.566 (<0.001)	0.471 (<0.001)	0.404 (<0.001)
CD8+ TIL	0.566 (<0.001)	-	0.418 (<0.001)	0.310 (<0.001)
FOXP3+ TIL	0.471 (<0.001)	0.418 (<0.001)	-	0.417 (<0.001)
PD-L1+ IC	0.404 (<0.001)	0.310 (<0.001)	0.417 (<0.001)	-

Data are presented as rho correlation coefficients calculated by Spearman's rank correlation test and p values in parentheses.

Supplementary Table S2. Summary of 6 cases with ipsilateral breast recurrence

No.	Extent of DCIS (cm)	Nuclear grade	HR	HER2	Node status	Surgery	Safety margin (cm)	Adjuvant radiation therapy	Time to recurrence (year)	Type of recurrent tumor
10	1.5	2	+	-	Nx	BCS	0.5	+	4.96	DCIS
23	2.0	3	-	-	Nx	BCS	0.4	+	2.79	IDC
41	1.6	3	+	-	Nx	BCS	1.0	+	4.24	DCIS
45	4.0	2	+	-	Nx	BCS	<0.1	+	6.32	IDC
81	2.7	2	+	-	Nx	BCS	0.9	+	3.78	DCIS
166	0.8	2	+	-	Nx	BCS	2.0	+	0.63	DCIS

BCS, breast conserving surgery

Supplementary Table S3. Clinicopathologic characteristics of DCIS (set 2)

Characteristic	No. (n=16)
Age at diagnosis, years	
Mean \pm standard deviation	53.5 \pm 12.8
Extent, cm	
Mean \pm standard deviation	4.3 \pm 4.7
Nuclear grade	
Low	0
Intermediate	6 (37.5)
High	10 (62.5)
Comedo-type necrosis	
Absent	8 (50.0)
Present	8 (50.0)
Microinvasion	
Present	12 (75.0)
Absent	4 (25.0)
Hormone receptor	
Positive	9 (56.3)
Negative	7 (43.8)
HER2 status	
Negative	11 (68.8)
Positive	5 (31.3)
Ki67 index	
Low (<10%)	4 (25.0)
High (\geq 10%)	12 (75.0)
P53 overexpression*	
Absent	7 (43.8)
Present	8 (50.0)
Subtype	
Luminal A	3 (18.8)
Luminal B	5 (31.2)
HER2+	6 (37.5)
Triple negative	2 (12.5)

*p53 expression was not evaluated in 1 case

Supplementary Table S4. Clinicopathologic characteristics of invasive carcinomas (set 2)

Characteristic	No. (n=32)
Age at diagnosis, years	
Mean \pm standard deviation	51.6 \pm 12.5
T stage	
T1	10 (31.3)
T2	22 (68.8)
T3	0 (0.0)
T4	0 (0.0)
Histologic grade	
Low (I & II)	6 (18.7)
High (III)	26 (81.3)
Lymph node metastasis*	
Absent	13 (40.6)
Present	17 (53.1)
Subtype	
Luminal A	7 (21.9)
Luminal B	9 (28.1)
HER2 positive	13 (40.6)
Triple negative	3 (9.4)
Hormone receptor	
Positive	16 (50.0)
Negative	16 (50.0)
HER2 amplification	
Absent	20 (62.5)
Present	12 (37.5)
Lymphovascular invasion	
Absent	10 (31.3)
Present	22 (68.8)
Ki-67 proliferation index	
<20%	11 (34.4)
\geq 20%	21 (65.6)
P53 Overexpression	
Absent	19 (59.4)
Present	12 (37.5)

*Node staging was not done in 2 cases

Supplementary Table S5. List of top 20 genes with significant fold change between DCIS and invasive carcinoma in ER-positive tumors

Gene	Log2 fold change	P-value	Adjusted p-value#
S100A8	2.25	0.00714	1.00
LAG3	2.03	0.00368	1.00
CXCL10	1.94	0.000903	0.727
CXCL9	1.90	0.00463	1.00
BIRC5	1.88	0.000352	0.727
PLAU	1.45	0.00116	0.798
CDK1	1.38	0.0016	0.965
HLA-DRA	1.30	0.00922	1.00
TFRC	1.21	0.000707	0.727
CXCR4	1.00	0.00823	1.00
F12	0.99	0.00382	1.00
GTF3C1	0.91	0.00193	1.00
BAX	0.40	0.00335	1.00
CFI	-0.67	0.00584	1.00
IL6R	-0.87	0.00322	1.00
MAP2K4	-0.93	0.000881	0.727
CCL18	-1.36	0.00634	1.00
CXCL1	-1.48	0.00723	1.00
CXCL2	-1.69	0.000754	0.727
LTF	-2.46	0.000688	0.727

DCIS includes pure DCIS and DCIS with microinvasion

p-values adjusted by Benjamini-Yekutieli procedure

Supplementary Table S6. List of top 20 genes with significant fold change between DCIS and invasive carcinoma in ER-negative tumors

Gene	Log2 fold change	P-value	Adjusted p-value#
CXCL10	3.44	0.00019	0.57
HLA-A	2.72	0.00429	1.00
IFITM1	2.61	0.000916	1.00
CXCL9	2.56	0.000334	0.57
APOE	2.04	0.00443	1.00
COL3A1	2.01	0.00518	1.00
CTSS	1.98	0.000354	0.57
SERPING1	1.90	0.00141	1.00
CCL5	1.89	0.00449	1.00
LCP1	1.78	0.00173	1.00
C1S	1.74	0.00123	1.00
PLAU	1.32	0.00314	1.00
PDGFRB	1.14	0.00288	1.00
GPI	1.05	0.00523	1.00
FCGR2A	0.98	0.00281	1.00
BMI1	0.94	0.00537	1.00
IFNAR2	0.86	0.0026	1.00
CD83	0.70	0.00366	1.00
TRAF3	0.61	0.00187	1.00
CSF3	-2.82	0.00453	1.00

DCIS includes pure DCIS and DCIS with microinvasion

p-values adjusted by Benjamini Y procedure

Supplementary Table S7. Clinicopathologic characteristics of DCIS (set 3)

Characteristic	No. (n=60)
Age at diagnosis, years	
Mean \pm standard deviation	50.9 \pm 10.7
Extent, cm	
Mean \pm standard deviation	4.3 \pm 2.4
Nuclear grade	
Low	4 (6.7)
Intermediate	16 (26.7)
High	40 (66.7)
Comedo-type necrosis	
Absent	29 (48.3)
Present	31 (51.7)
Microinvasion	
Present	21 (35.0)
Absent	39 (65.0)
Hormone receptor	
Positive	30 (50.0)
Negative	30 (50.0)
HER2 status	
Negative	29 (48.3)
Positive	31 (51.7)
Ki67 index	
Low (<10%)	24 (40.0)
High (\geq 10%)	36 (60.0)
P53 overexpression	
Absent	37 (61.7)
Present	23 (38.3)
Subtype	
Luminal A	15 (25.0)
Luminal B	15 (25.0)
HER2+	22 (36.7)
Triple negative	8 (13.3)

Supplementary Table S8. Clinicopathologic characteristics of invasive carcinomas (set 3)

Characteristic	No. (n=60)
Age at diagnosis, years	
Mean \pm standard deviation	53.4 \pm 13.06
T stage	
T1	23 (38.3)
T2	37 (61.7)
T3	0 (0.0)
T4	0 (0.0)
Histologic grade	
Low (I & II)	23 (38.3)
High (III)	37 (61.7)
Lymph node metastasis	
Absent	45 (75.0)
Present	37 (61.7)
Subtype	
Luminal A	25 (41.7)
Luminal B	5 (8.3)
HER2 positive	10 (16.7)
Triple negative	20 (33.3)
Hormone receptor	
Positive	30 (50.0)
Negative	16 (50.0)
HER2 amplification	
Absent	45 (75.0)
Present	15 (25.0)
Lymphovascular invasion	
Absent	36 (60.0)
Present	24 (40.0)
Ki-67 proliferation index	
<20%	23 (38.3)
\geq 20%	37 (61.7)
P53 Overexpression	
Absent	38 (63.3)
Present	22 (36.7)

Supplementary Table S9. Clinicopathologic characteristics of DCIS (set 4)

Characteristic	No. (n=223)
Age at diagnosis, years	
Mean \pm standard deviation	47.0 \pm 10.3
Relapse free survival, years	
Mean \pm standard deviation	4.9 \pm 2.9
Extent, cm	
Mean \pm standard deviation	3.5 \pm 2.5
Nuclear grade	
Low	11 (4.9)
Intermediate	105 (47.1)
High	107 (48.0)
Comedo-type necrosis	
Absent	146 (65.5)
Present	77 (34.5)
Microinvasion	
Present	59 (26.5)
Absent	164 (73.5)
Estrogen receptor (1%)	
Positive	171 (76.7)
Negative	52 (23.3)
Progesterone receptor (1%)	
Positive	159 (71.3)
Negative	64 (28.7)
HER2 status	
Negative	170 (76.2)
Positive	53 (23.8)
Ki67 index	
Low (<10%)	143 (64.1)
High (\geq 10%)	80 (35.9)
P53 overexpression	
Absent	183 (82.1)
Present	40 (17.9)
Subtype	
Luminal A	136 (61.0)
Luminal B	37 (16.6)
HER2+	30 (13.5)
Triple negative	20 (9.0)
Adjuvant radiation therapy	
Not received	102 (45.7)
Received	121 (54.3)
Adjuvant hormonal therapy	
Not received	138 (61.9)
Received	85 (38.1)

Unless specified, number in parenthesis indicates percentage.

Supplementary Table S10. Clinicopathologic characteristics of invasive carcinomas (set 4)

Characteristic	No. (n=372)
Age at diagnosis, years	
Mean \pm standard deviation	50.1 \pm 11.8
Follow up, years (diseases free survival)	
Mean \pm standard deviation	10.7 \pm 4.7
T stage	
T1	156 (41.9)
T2	195 (52.4)
T3	13 (3.5)
T4	8 (2.2)
N stage	
N0	202 (54.3)
N1	102 (27.4)
N2	35 (9.4)
N3	33 (8.9)
Histologic subtype	
Invasive carcinoma of no special type	339 (91.1)
Mucinous carcinoma	12 (3.2)
Metaplastic carcinoma	10 (2.7)
Others	11 (3.0)*
Histologic grade	
Low	66 (17.7)
Intermediate	124 (33.3)
High	182 (48.9)
Lymphovascular invasion	
Absent	205 (55.1)
Present	167 (44.9)
Estrogen receptor	
Positive	257 (69.1)
Negative	115 (30.9)
Progesterone receptor	
Positive	227 (61.0)
Negative	145 (39.0)
HER2 status	
Negative	297 (79.8)
Positive	75 (20.2)
Ki67 index	
Low (<20%)	214 (57.5)
High (\geq 20%)	158 (42.5)
P53 overexpression	
Absent	281 (75.5)
Present	91 (24.5)
Subtype	
Luminal A	176 (47.3)
Luminal B	81 (21.8)
HER2+	38 (10.2)
Triple negative	77 (20.7)
Neo-adjuvant chemotherapy	
Not received	340 (91.4)
Received	32 (8.6)
Adjuvant chemotherapy*	
Not received	65 (17.5)
Received	301 (80.9)
Adjuvant HER2-targeted therapy*	
Not received	340 (91.4)
Received	26 (7.0)
Adjuvant radiation therapy*	
Not received	149 (40.7)
Received	217 (59.3)
Adjuvant hormonal therapy*	
Not received	115 (31.4)
Received	251 (68.6)

Unless specified, number in parenthesis indicate percentage.

*Information on adjuvant therapy could not be assessed in 6 cases due to follow-up loss.

Supplementary Table S11. Relationship between CXCL10 expression and clinicopathologic features of DCIS

Clinicopathologic feature	CXCL10		<i>p</i> value
	Negative	Positive	
Extent			0.722
<3.8cm	114 (56.4)	11 (52.4)	
≥3.8cm	88 (43.6)	10 (47.6)	
Nuclear grade			0.441
Low	11 (5.4)	0 (0)	
Intermediate	96 (47.5)	9 (42.9)	
High	95 (47.0)	12 (57.1)	
Comedo-type necrosis			0.399
Absent	134 (66.3)	12 (57.1)	
Present	68 (33.7)	9 (42.9)	
Microinvasion			0.453
Present	52 (25.7)	7 (11.9)	
Absent	150 (74.3)	14 (66.7)	
ER			0.589
Positive	156 (77.2)	15 (71.4)	
Negative	46 (22.8)	6 (28.6)	
PR			0.132
Positive	147 (72.8)	12 (57.1)	
Negative	55 (27.2)	9 (42.9)	
HER2 status			0.675
Negative	155 (76.7)	15 (71.4)	
Positive	47 (23.3)	6 (28.6)	
Ki67 index			0.824
Low (<10%)	130 (64.4)	13 (61.9)	
High (≥10%)	72 (35.6)	8 (38.1)	
P53 overexpression			0.548
Absent	167 (82.7)	16 (76.2)	
Present	35 (17.3)	5 (23.8)	
Subtype			0.487
Luminal A	124 (61.4)	12 (57.1)	
Luminal B	34 (16.8)	3 (14.3)	
HER2+	25 (12.4)	5 (23.8)	
Triple negative	19 (9.4)	1 (4.8)	

P values are calculated by Chi-square or Fisher's exact test. Number in parenthesis indicates percentage.

Supplementary Table S12. Relationship between CXCL10 expression and clinicopathologic features of invasive carcinoma

Clinicopathologic features	CXCL10		<i>p</i> value
	Negative	Positive	
T stage			0.057
T1	271 (93.1)	80 (98.8)	
T2-T4	20 (6.9)	1 (1.2)	
N stage			0.129
N0	152 (52.2)	50 (24.8)	
N1-N3	139 (47.8)	31 (38.3)	
Histologic grade			<0.001
Low	61 (21.0)	5 (6.2)	
Intermediate	107 (36.8)	17 (21.0)	
High	123 (42.3)	59 (72.8)	
LVI			0.551
Absent	158 (54.3)	47 (58.0)	
Present	133 (45.7)	34 (42.0)	
ER			<0.001
Positive	224 (77.0)	33 (40.7)	
Negative	67 (23.0)	48 (59.3)	
PR			<0.001
Positive	197 (67.7)	30 (37.0)	
Negative	94 (32.3)	51 (63.0)	
HER2 status			0.144
Negative	237 (81.4)	60 (74.1)	
Positive	54 (18.6)	21 (25.9)	
Ki67 index			<0.001
Low (<20%)	188 (64.6)	26 (32.1)	
High (≥20%)	103 (35.4)	55 (67.9)	
P53 overexpression			0.001
Absent	231 (79.4)	50 (61.7)	
Present	60 (20.6)	31 (38.3)	
Subtype			<0.001
Luminal A	155 (53.3)	22 (27.2)	
Luminal B	74 (25.4)	13 (16.0)	
HER2+	20 (6.9)	15 (18.5)	
Triple negative	42 (14.4)	31(38.3)	

P values are calculated by Chi-square or Fisher's exact test. Number in parenthesis indicates percentage.

LVI, lymphovascular invasion

Bibliography

1. Koh, V.C., et al., *Characteristics and behaviour of screen-detected ductal carcinoma in situ of the breast: comparison with symptomatic patients*. Breast Cancer Res Treat, 2015. **152**(2): p. 293-304.
2. Erbas, B., et al., *The natural history of ductal carcinoma in situ of the breast: a review*. Breast Cancer Res Treat, 2006. **97**(2): p. 135-44.
3. Choi, Y., et al., *Epithelial-mesenchymal transition increases during the progression of in situ to invasive basal-like breast cancer*. Hum Pathol, 2013. **44**(11): p. 2581-9.
4. Swann, J.B. and M.J. Smyth, *Immune surveillance of tumors*. J Clin Invest, 2007. **117**(5): p. 1137-46.
5. Chen, X.Y., et al., *Prognostic role of immune infiltrates in breast ductal carcinoma in situ*. Breast Cancer Res Treat, 2019.
6. Kroemer, G., et al., *Natural and therapy-induced immunosurveillance in breast cancer*. Nat Med, 2015. **21**(10): p. 1128-38.
7. Luen, S., et al., *The genomic landscape of breast cancer and its interaction with host immunity*. Breast, 2016. **29**: p. 241-50.
8. Herbst, R.S., et al., *Predictive correlates of response to the anti-PD-L1 antibody MPDL3280A in cancer patients*. Nature, 2014. **515**(7528): p. 563-7.
9. Denkert, C., et al., *Tumor-associated lymphocytes as an independent predictor of response to neoadjuvant chemotherapy in breast cancer*. J Clin Oncol, 2010. **28**(1): p. 105-13.
10. Loi, S., et al., *Prognostic and predictive value of tumor-infiltrating lymphocytes in a phase III randomized adjuvant breast cancer trial in node-positive breast cancer comparing the addition of docetaxel to doxorubicin with doxorubicin-based chemotherapy: BIG 02-98*. J Clin Oncol, 2013. **31**(7): p. 860-7.
11. Mohammed, Z.M., et al., *The relationship between components of tumour inflammatory cell infiltrate and clinicopathological factors and survival in patients with primary operable invasive ductal breast cancer*. Br J Cancer, 2012. **107**(5): p. 864-73.
12. Mahmoud, S.M., et al., *Tumor-infiltrating CD8+ lymphocytes predict clinical outcome in breast cancer*. J Clin Oncol, 2011. **29**(15): p. 1949-55.
13. Seo, A.N., et al., *Tumour-infiltrating CD8+ lymphocytes as an independent predictive factor for pathological complete response to primary systemic therapy in breast cancer*. Br J Cancer, 2013. **109**(10): p. 2705-13.
14. Chung, Y.R., et al., *Prognostic value of tumor infiltrating lymphocyte subsets in breast cancer depends on hormone receptor status*. Breast Cancer Res Treat, 2017. **161**(3): p. 409-420.
15. Toss, M.S., et al., *Prognostic significance of tumor-infiltrating lymphocytes in ductal carcinoma in situ of the breast*. Mod Pathol, 2018. **31**(8): p. 1226-1236.
16. Hendry, S., et al., *Relationship of the Breast Ductal Carcinoma In Situ Immune Microenvironment with Clinicopathological and Genetic Features*. Clin Cancer Res, 2017. **23**(17): p. 5210-5217.
17. Campbell, M.J., et al., *Characterizing the immune microenvironment in high-risk ductal carcinoma in situ of the breast*. Breast Cancer Res Treat, 2017. **161**(1): p. 17-28.
18. Miligy, I., et al., *Prognostic significance of tumour infiltrating B lymphocytes in breast ductal carcinoma in situ*. Histopathology, 2017. **71**(2): p. 258-268.
19. Semeraro, M., et al., *The ratio of CD8(+)/FOXP3 T lymphocytes infiltrating breast tissues predicts the relapse of ductal carcinoma in situ*. Oncoimmunology, 2016. **5**(10): p. e1218106.
20. Thompson, E., et al., *The immune microenvironment of breast ductal carcinoma in*

- situ. *Mod Pathol*, 2016. **29**(3): p. 249-58.
21. Ubago, J.M., et al., *The PD-1/PD-L1 Axis in HER2+ Ductal Carcinoma In Situ (DCIS) of the Breast*. *Am J Clin Pathol*, 2019. **152**(2): p. 169-176.
22. Lv, S., et al., *Functional CD3(+)CD8(+)PD1(-) T Cell Accumulation and PD-L1 Expression Increases During Tumor Invasion in DCIS of the Breast*. *Clin Breast Cancer*, 2019.
23. Luster, A.D., *Chemokines--chemotactic cytokines that mediate inflammation*. *N Engl J Med*, 1998. **338**(7): p. 436-45.
24. Proudfoot, A.E., *Chemokine receptors: multifaceted therapeutic targets*. *Nat Rev Immunol*, 2002. **2**(2): p. 106-15.
25. Karin, N. and H. Razon, *Chemokines beyond chemo-attraction: CXCL10 and its significant role in cancer and autoimmunity*. *Cytokine*, 2018. **109**: p. 24-28.
26. Hendry, S., et al., *Assessing Tumor-infiltrating Lymphocytes in Solid Tumors: A Practical Review for Pathologists and Proposal for a Standardized Method From the International Immunooncology Biomarkers Working Group: Part 1: Assessing the Host Immune Response, TILs in Invasive Breast Carcinoma and Ductal Carcinoma In Situ, Metastatic Tumor Deposits and Areas for Further Research*. *Adv Anat Pathol*, 2017. **24**(5): p. 235-251.
27. Dieci, M.V., et al., *Update on tumor-infiltrating lymphocytes (TILs) in breast cancer; including recommendations to assess TILs in residual disease after neoadjuvant therapy and in carcinoma in situ: A report of the International Immuno-Oncology Biomarker Working Group on Breast Cancer*. *Semin Cancer Biol*, 2018. **52**(Pt 2): p. 16-25.
28. Stanton, S.E., S. Adams, and M.L. Disis, *Variation in the Incidence and Magnitude of Tumor-Infiltrating Lymphocytes in Breast Cancer Subtypes: A Systematic Review*. *JAMA Oncol*, 2016. **2**(10): p. 1354-1360.
29. Pruneri, G., et al., *The prevalence and clinical relevance of tumor-infiltrating lymphocytes (TILs) in ductal carcinoma in situ of the breast*. *Ann Oncol*, 2017. **28**(2): p. 321-328.
30. Beguinot, M., et al., *Analysis of tumour-infiltrating lymphocytes reveals two new biologically different subgroups of breast ductal carcinoma in situ*. *BMC Cancer*, 2018. **18**(1): p. 129.
31. Hussein, M.R. and H.I. Hassan, *Analysis of the mononuclear inflammatory cell infiltrate in the normal breast, benign proliferative breast disease, in situ and infiltrating ductal breast carcinomas: preliminary observations*. *J Clin Pathol*, 2006. **59**(9): p. 972-7.
32. Lal, A., et al., *FOXP3-positive regulatory T lymphocytes and epithelial FOXP3 expression in synchronous normal, ductal carcinoma in situ, and invasive cancer of the breast*. *Breast Cancer Res Treat*, 2013. **139**(2): p. 381-90.
33. Kim, H.J. and H. Cantor, *CD4 T-cell subsets and tumor immunity: the helpful and the not-so-helpful*. *Cancer Immunol Res*, 2014. **2**(2): p. 91-8.
34. Schmidt, M., et al., *Prognostic impact of CD4-positive T cell subsets in early breast cancer: a study based on the FinHer trial patient population*. *Breast Cancer Res*, 2018. **20**(1): p. 15.
35. Hammerl, D., et al., *Breast cancer genomics and immuno-oncological markers to guide immune therapies*. *Semin Cancer Biol*, 2018. **52**(Pt 2): p. 178-188.
36. Liu, S., et al., *Prognostic significance of FOXP3+ tumor-infiltrating lymphocytes in breast cancer depends on estrogen receptor and human epidermal growth factor receptor-2 expression status and concurrent cytotoxic T-cell infiltration*. *Breast Cancer Res*, 2014. **16**(5): p. 432.
37. Goldfarb, R.H. and L.A. Liotta, *Proteolytic enzymes in cancer invasion and metastasis*. *Semin Thromb Hemost*, 1986. **12**(4): p. 294-307.
38. Polyak, K. and M. Hu, *Do myoepithelial cells hold the key for breast tumor progression?* *J Mammary Gland Biol Neoplasia*, 2005. **10**(3): p. 231-47.

39. Man, Y.G. and Q.X. Sang, *The significance of focal myoepithelial cell layer disruptions in human breast tumor invasion: a paradigm shift from the "protease-centered" hypothesis*. Exp Cell Res, 2004. **301**(2): p. 103-18.
40. Hwang, E.S., et al., *Patterns of chromosomal alterations in breast ductal carcinoma in situ*. Clin Cancer Res, 2004. **10**(15): p. 5160-7.
41. Schoenborn, J.R. and C.B. Wilson, *Regulation of interferon-gamma during innate and adaptive immune responses*. Adv Immunol, 2007. **96**: p. 41-101.
42. Tokunaga, R., et al., *CXCL9, CXCL10, CXCL11/CXCR3 axis for immune activation - A target for novel cancer therapy*. Cancer Treat Rev, 2018. **63**: p. 40-47.
43. Yang, X., et al., *Targeted in vivo expression of IFN-gamma-inducible protein 10 induces specific antitumor activity*. J Leukoc Biol, 2006. **80**(6): p. 1434-44.
44. Mulligan, A.M., et al., *Tumoral lymphocytic infiltration and expression of the chemokine CXCL10 in breast cancers from the Ontario Familial Breast Cancer Registry*. Clin Cancer Res, 2013. **19**(2): p. 336-46.
45. Barash, U., et al., *Heparanase enhances myeloma progression via CXCL10 downregulation*. Leukemia, 2014. **28**(11): p. 2178-87.
46. Ma, X., et al., *CXCR3 expression is associated with poor survival in breast cancer and promotes metastasis in a murine model*. Mol Cancer Ther, 2009. **8**(3): p. 490-8.
47. Kawada, K., et al., *Pivotal role of CXCR3 in melanoma cell metastasis to lymph nodes*. Cancer Res, 2004. **64**(11): p. 4010-7.
48. Ejaeidi, A.A., et al., *Hormone receptor-independent CXCL10 production is associated with the regulation of cellular factors linked to breast cancer progression and metastasis*. Exp Mol Pathol, 2015. **99**(1): p. 163-72.
49. Zipin-Roitman, A., et al., *CXCL10 promotes invasion-related properties in human colorectal carcinoma cells*. Cancer Res, 2007. **67**(7): p. 3396-405.
50. Datta, D., et al., *Ras-induced modulation of CXCL10 and its receptor splice variant CXCR3-B in MDA-MB-435 and MCF-7 cells: relevance for the development of human breast cancer*. Cancer Res, 2006. **66**(19): p. 9509-18.
51. Chuan, T., T. Li, and C. Yi, *Identification of CXCR4 and CXCL10 as Potential Predictive Biomarkers in Triple Negative Breast Cancer (TNBC)*. Med Sci Monit, 2020. **26**: p. e918281.
52. Loetscher, M., et al., *Chemokine receptor specific for IP10 and mig: structure, function, and expression in activated T-lymphocytes*. J Exp Med, 1996. **184**(3): p. 963-9.
53. Groom, J.R. and A.D. Luster, *CXCR3 ligands: redundant, collaborative and antagonistic functions*. Immunol Cell Biol, 2011. **89**(2): p. 207-15.
54. Li, C.X., et al., *CXCL10/CXCR3 signaling mobilized-regulatory T cells promote liver tumor recurrence after transplantation*. J Hepatol, 2016. **65**(5): p. 944-952.
55. Lunardi, S., et al., *IP-10/CXCL10 attracts regulatory T cells: Implication for pancreatic cancer*. Oncoimmunology, 2015. **4**(9): p. e1027473.
56. Zohar, Y., et al., *CXCL11-dependent induction of FOXP3-negative regulatory T cells suppresses autoimmune encephalomyelitis*. J Clin Invest, 2018. **128**(3): p. 1200-1201.
57. Peng, W., et al., *PD-1 blockade enhances T-cell migration to tumors by elevating IFN-γ inducible chemokines*. Cancer Res, 2012. **72**(20): p. 5209-18.
58. Zhang, C., et al., *CXCL9/10/11, a regulator of PD-L1 expression in gastric cancer*. BMC Cancer, 2018. **18**(1): p. 462.
59. Chheda, Z.S., et al., *Chemoattractant Receptors BLT1 and CXCR3 Regulate Antitumor Immunity by Facilitating CD8+ T Cell Migration into Tumors*. J Immunol, 2016. **197**(5): p. 2016-26.
60. Sheu, B.C., et al., *Clinical significance of tumor-infiltrating lymphocytes in neoplastic progression and lymph node metastasis of human breast cancer*. Breast,

2008. **17**(6): p. 604-10.
61. Gil Del Alcazar, C.R., et al., *Immune Escape in Breast Cancer During In Situ to Invasive Carcinoma Transition*. Cancer Discov, 2017. **7**(10): p. 1098-1115.
 62. Reynders, N., et al., *The Distinct Roles of CXCR3 Variants and Their Ligands in the Tumor Microenvironment*. Cells, 2019. **8**(6).
 63. Lu, B., et al., *Structure and function of the murine chemokine receptor CXCR3*. Eur J Immunol, 1999. **29**(11): p. 3804-12.
 64. Liu, M., S. Guo, and J.K. Stiles, *The emerging role of CXCL10 in cancer (Review)*. Oncol Lett, 2011. **2**(4): p. 583-589.

국문 초록

서론: 유방 관상피내암종의 면역미세환경과 그 중요성은 아직까지 잘 확립되지 않았다. 본 연구에서는 관상피내암종과 침윤암종의 종양침윤 림프구 아형, PD-L1 양성 면역세포 침윤 및 면역관련 유전자 발현을 비교분석하여 관상피내암종의 진행에 면역미세환경이 어떠한 역할을 하는지 알아보고자 하였다.

재료 및 방법: 순수 관상피내암종, 미세침윤암종, 침윤암종으로 이루어진 세 개 그룹의 유방암 조직이 사용되었다. CD4, CD8, FOXP 양성 림프구 및 PD-L1 양성 면역세포는 tissue microarray를 이용하여 면역조직화학염색을 통해 분석하였다. Nanostring nCounter를 사용한 면역 프로파일링을 통하여 CXCL10이 관상피내암종과 침윤성암종에서 가장 큰 발현 차이를 보이는 유전자임을 확인하였고, 실시간 중합 효소 연쇄 반응 및 면역조직화학염색을 통하여 이를 검증하였다. 또한 CXCL10의 발현과 임상병리학적 특징 및 종양 침윤성 림프구 아형과의 상관관계를 분석하였다.

결과: 모든 면역세포 침윤은 호르몬 수용체 발현 여부와 관계없이 관상피내암종보다 침윤암종에서 높게 관찰되었다. 관상피내암종을 동반한 침윤암종에서 면역세포의 침윤은 관상피내암종 부분보다 침윤암종 부분에서 증가하였으나, 호르몬 수용체 음성인 경우 CD4 양성 림프구는 두 군간에 차이를 보이지 않았다. 순수 관상피내암종, 미세침윤암종에 동반된 관상피내암종, 침윤암종에 동반된 관상피내암종 세 군을 비교분석 하였을 때, 호르몬 수용체 음성 유방암에서는 CD4 양성 림프구 침윤이 순수 관상피내암종, 미세침윤암종에 동반된 관상피내암종, 침윤암종에 동반된 관상피내암종 순서로 점차 증가하였고, 호르몬 수용체 양성 유방암에서는 FOXP3 양성 림프구가 순수 관상피내암종에 비해 침윤암종에 동반된 관상피내암종에서 유의하게 증가하였다. FOXP3 양성 림프구 침윤과

PD-L1 양성 면역세포 침윤의 증가는 순수 관상피내암종 환자에서 종양의 재발과 연관성이 있었다. CXCL10 mRNA의 발현은 전체군과 호르몬 수용체 음성군에서 관상피내암종보다 침윤암종에서 더 높게 나타났다. 특히 호르몬 수용체 음성인 경우 순수 관상피내암종에 비하여 침윤암종에 동반된 관상피내암종에서 CXCL10 mRNA 발현이 증가하였다. 또한, CXCL10 mRNA 발현은 관상피내암종과 침윤암종 모두에서 면역세포 침윤과 양의 상관관계를 보였다. CXCL10 양성종양은 일반적으로 CXCL10 음성 종양에 비해 CD8 양성 림프구와 FOXP3 양성 림프구 및 PD-L1 양성 면역세포의 침윤이 증가하는 경향을 보였다. 그러나 호르몬 수용체 발현 여부에 따라 침윤 양상의 차이를 보였다.

결론: 본 연구는 순수 관상피내암종, 미세침윤암종, 침윤암종의 면역미세환경이 호르몬 수용체 발현 여부에 따라 면역세포 아형의 침윤에서 크게 차이를 보였다. 또한 CXCL10 발현이 관상피내암종과 침윤암종에서의 면역세포 침윤의 차이와 연관되어 있다는 것을 보임으로써 면역세포 침윤 및 CXCL10 발현의 변화가 관상피내암종에서 침윤암종으로의 진행에 연관되어 있음을 제시하였다.

주요어: 관상피내암종, 침윤성 유방암, 종양 면역미세환경, 종양침윤림프구, CXCL10

학번: 2016-27715